NATIONAL AERONAUTICS AND SPACE ADMINISTRATION

Technical Report 32-1330

Experimental Evaluation of a Throttlable Impinging-Sheet Injector with Earth-Storable Propellants

(Title Unclassified)

Robert W. Riebling

JET PROPULSION LABORATORY
CALIFORNIA INSTITUTE OF TECHNOLOGY
PASADENA, CALIFORNIA

October 15, 1968

NATIONAL AERONAUTICS AND SPACE ADMINISTRATION

Technical Report 32-1330

Experimental Evaluation of a Throttlable Impinging-Sheet Injector with Earth-Storable Propellants

(Title Unclassified)

Robert W. Riebling

Copy No. 255

JET PROPULSION LABORATORY
CALIFORNIA INSTITUTE OF TECHNOLOGY
PASADENA, CALIFORNIA

October 15, 1968

TECHNICAL REPORT 32-1330

Prepared Under Contract No. NAS 7-100
National Aeronautics & Space Administration

(U) Preface

The work described in this report was performed by the Propulsion Division of the Jet Propulsion Laboratory.

(U) Acknowledgment

The author wishes to acknowledge with sincere thanks the contributions of the following persons to this investigation. Mr. Bruce H. Johnson, formerly of the Jet Propulsion Laboratory, conceived the impinging-sheet concept, and Mr. David D. Evans conducted the initial single-element impinging-sheet injector firings. It was the promise shown by these early devices that led to the present evaluation of a multiple-element, pre-prototype injector.

The author is also indebted to Mr. Allan R. McDougal for his role in the mechanical design of the apparatus, and to Mr. Donald L. Bond who conducted the firings at the Edwards Test Facility. Mr. Richard N. Porter, formerly of this Laboratory, originally suggested the discrete-element throttling technique.

(U) Contents

(U) Contents (contd)

Tables

Figures

(U) Contents (contd)

Figures (contd)

Abstract

(U) A multiple-element, unlike-impinging-sheet injector was designed, fabricated, and fired with three earth-storable propellant combinations. Combustion efficiencies were measured during throttling of the injector by two separate techniques: pressure/area-step and discrete-element. During firings, in which the mixture ratio and characteristic chamber length were varied, combustion efficiencies were also measured. Combustion stability and smoothness were monitored; a limited number of chamber and nozzle wall heat-flux measurements were made.

(C) The results indicated that impinging-sheet injectors of this type are competitive with contemporary impinging-jet designs as to the efficiency and stability of combustion attainable, and offer a marked improvement in the smoothness of combustion realizable with hydrazine fuel. Furthermore, they may be throttled, operated at off-mixture ratio conditions, and fired with several different propellant combinations within the same general chemical family, without appreciable degradation in combustion efficiency.

(U) When fired with hydrazine and monomethylhydrazine, maximum density fuming nitric acid appeared competitive with N_2O_4 as to combustion efficiency, stability, and smoothness.

(U) Injection elements mounted external to the injector face exhibited rather poor durability, especially during throttling, when the flow of propellants to them was cut off. Installation of the elements within the injector face (a "buried" configuration) might be desirable for future applications.

Experimental Evaluation of a Throttlable Impinging-Sheet Injector with Earth-Storable Propellants

I. Introduction

(C) One objective of the Advanced Liquid Propulsion Systems Program was the development of a restartable spacecraft rocket engine injector in the 2000–4000-lbf thrust class for use with earth-storable propellants, such as nitrogen tetroxide (N_2O_4) and hydrazine (N_2H_4). It was required that such an injector have a high combustion efficiency (at least 95% of the theoretically attainable shifting equilibrium characteristic velocity, c^*, at full thrust), and provide a predictable heat transfer environment compatible with chamber and nozzle wall materials, such as pyrolytic graphite or one of its alloys. In addition, it was desirable that the injector be continuously throttlable over about a 10–1 range of thrust without significant loss in combustion efficiency. Several previous attempts to meet these goals met with difficulties owing to the extreme reactivity of the N_2O_4–N_2H_4 combination, and to the tendency of the N_2H_4 to undergo rapid thermal decomposition in certain regions, often initiating combustion instability.

(C) With the evolution of the 25-lbf thrust impinging-sheet injector element, it became evident that a higher-thrust injector, composed of multiple elements, would have a high probability of success. At the 2000-lbf thrust (at altitude) scale such an injector was designed and fabricated. This report will describe that injector, and present the results of an experimental program conducted to: (1) demonstrate the feasibility of JPL's impinging-sheet injection concept in multi-element configurations, (2) evaluate several promising candidate throttling techniques, and (3) evaluate several other earth-storable propellant combinations.

II. Apparatus

A. Injector

(C) To achieve predictable and reproducible performance, heat transfer, and dynamic stability characteristics in an injector in the 2000-lbf thrust class, it is necessary to control the distribution of propellant mass flux and mixture ratio across the injector face (Refs. 1–5). Though attractive from the standpoint of simplicity, a single large injection element could not provide the necessary distributions of mass flux and mixture ratio. Therefore, a multiplicity of smaller elements was required. By using a sufficient number of identical elements with reproducible hydraulic characteristics, mass flux and mixture ratio distributions can be controlled by arrangement of the injection pattern alone.

(U) The injection element selected was the unlike-impinging sheet configuration conceived (Fig. 1) at the Jet Propulsion Laboratory. In this concept, jets issuing from round orifices are introduced *tangentially* onto curved deflector surfaces, where they form thin, relatively flat liquid sheets. (Typical sheet thicknesses are of the order of 0.005–0.010 in.) The use of thin sheets in rocket injectors is not new. Crude versions of the concept, in which the sheets were formed from slots or by *non-tangential* impingement of jets on "splash plates," are to be found in early literature. Even the tangential impingement technique (Fig. 1) has been used for some time in commercially available[1] spray nozzles. However, forming sheets in this manner for rocket engine injectors is an innovation that appears quite promising, because of the degree of control it affords over the sheet properties.

(U) Although impinging-sheet elements of this type are still relatively new, considerable information to aid in the understanding of their functioning is already available. For example, the formation and properties of individual sheets has been studied in some detail (Ref. 6). The dimensions, spatial orientation, and distributions of mass flux, velocity, and momentum can be related to deflector and orifice geometry. The geometrical relationships, which must be satisfied to assure proper dimensional matching of the sheets along their impingement line, have been worked out and are reported in Ref. 7. Cold-flow studies have been conducted to determine the effects of element geometry, propellant physical properties, and propellant momentum ratio on the degrees of mixing (Ref. 8), and atomization (Ref. 9) attained in the spray from single impinging-sheet injection elements under nonreactive conditions.

[1](U) Spraying Systems Co., 3201 Randolph Street, Bellwood, Ill.; Bete Fog Nozzle Inc., 309 Wells Street, Greenfield, Mass., etc.

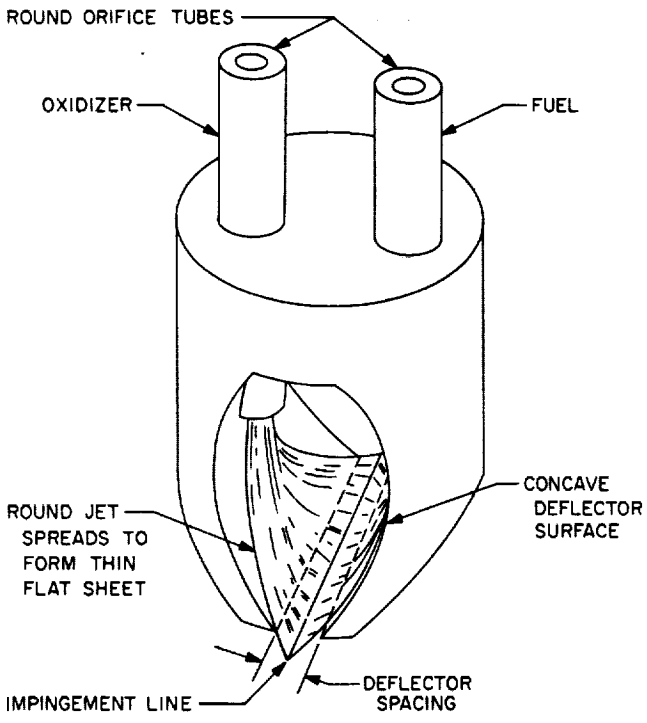

(U) Fig. 1. Typical impinging-sheet injector element

(C) Unlike-impinging sheets are less susceptible to the disrupting effects of rapid liquid-phase reactions on the primary propellant mixing process than unlike-impinging jets at a given level of thrust per element (Ref. 10). A series of test firings of single impinging-sheet elements at the 25-lbf thrust level (Ref. 11) indicated that this kind of element could be throttled over a fairly wide range by injection pressure variation without any appreciable degradation in c^* efficiency. Another series (Ref. 12) established the optimum values of impingement angle, deflector spacing, and element geometry for maximizing c^* efficiency. In addition, it was felt that impinging sheets would be less sensitive to the accuracy of stream alignment (and therefore to manufacturing tolerances), and could provide a degree of "film-cooling" to the injector face not attainable with conventional impinging-jet designs.

(U) The elements used in the present study had equal fuel and oxidizer orifice diameters, because these give equal injection pressure drops with N_2O_4/N_2H_4 at the design mixture ratio of 1.2. Orifice construction was of Type 321 stainless steel. For these propellants and this mixture ratio, equal diameters also fulfill the optimum mixing criterion for unlike-impinging jets (Ref. 13) which, in the absence of better information, was assumed to hold for unlike-impinging sheets as well. (Subsequently, the work of Ref. 8 showed that the degree of mixing attained in the nonreactive spray from a pair of impinging sheets was quite insensitive to stream momentum ratio, so that the mixing criterion does not seem to be of great importance for sheet injectors.)

(U) The fuel and oxidizer deflectors were identical, since the properties of an individual sheet are virtually independent of the propellants' physical properties (Ref. 6). The deflectors had radii of 0.278 in. and turned each stream through an angle of 49 deg., so that the sheets impinged at an angle of approximately 93 deg. (The sheets

do not leave the deflectors quite tangentially, so the impingment angle was not exactly twice the deflector angle.) Two complements of deflectors were fabricated: one lot of 78 elements was made of Type 321 stainless steel, and the second of TZM molybdenum. The steel deflectors, manufactured by conventional machining techniques, had a finish of 16 μin. (rms) on their flow surfaces. To minimize costs, the molybdenum deflectors were made by electrodischarge machining and had a surface finish of about 50 μin. rms. However, it should be pointed out that the two machining processes produced quite different surface characteristics. Figure 2 shows photomacrographs of surfaces similar to those used on the deflectors, except that the surfaces in Fig. 2 are flat to facilitate their photography. The ground surface consists of long, parallel grooves, whereas the electrodischarge-machined surface is pitted. The spacing between deflectors (Fig. 1) was 0.050 in. and a propellant momentum ratio of unity made the resultant momentum vector of each fan parallel to the longitudinal axis of the element.

(U) To assure that each injector element provided an identical and reproducible mass flow and velocity, the manifolding and feed system (shown schematically in Fig. 3) were made a part of the injector. The manifold was designed to maintain very low (less than 3 ft/s) crossflow velocities and to provide each orifice entry with an almost identical pressure and velocity environment. Each orifice was fed individually by a long, contoured-entry feeder tube, which passed through the wall of the injection head from the rear. This allowed more freedom in orifice pattern layout than conventional designs, which used radially-drilled feeder passages fed by an annular manifold. A gradual transition was made from the 0.086-in.-diam feeder tubes to the 0.038-in.-diam orifices, across which most of the injection pressure drop (75 psid on both fuel and oxidizer sides at full thrust) occurred. The length-to-diameter ratios of the feeder and orifice tubes were 40:1 (or greater, depending on location) and 25:1, respectively. Figure 4 shows the injector (with manifold removed) revealing the arrangement of the feeder tubes. Construction of the remainder of the injector was of Type 347 stainless steel, including the feeder tubes, which

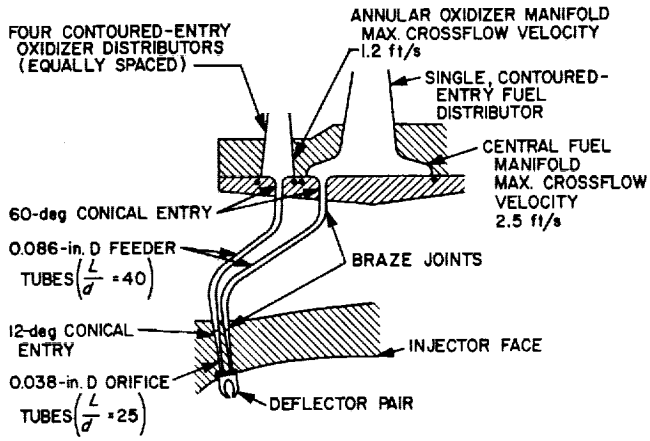

(U) Fig. 3. Injector manifolding and orifice feed system

(a) 16-μin. GROUND SURFACE

(b) 50-μin. ELECTRODISCHARGE-MACHINED SURFACE

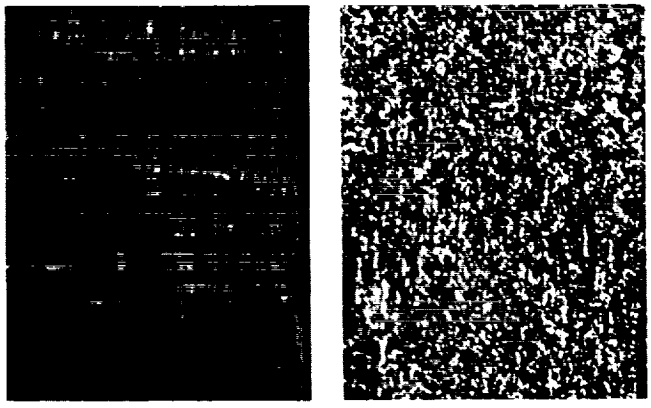

(U) Fig. 2. Photomacrographs of machined surfaces similar to those on deflectors

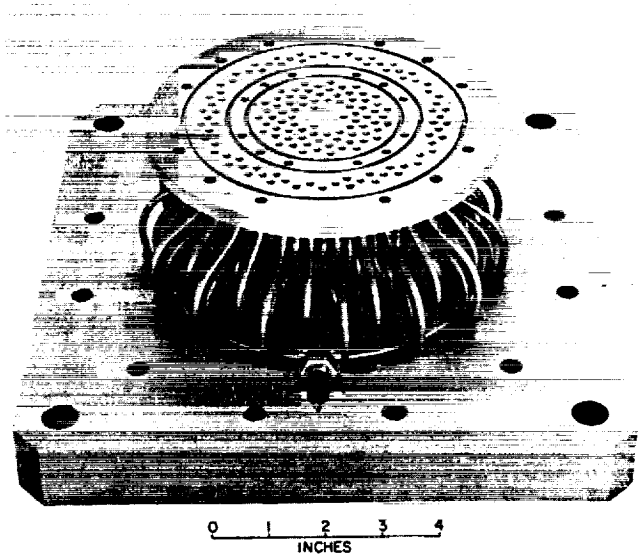

(U) Fig. 4. Manifold side of 2000-lbf thrust, 78-element, impinging-sheet injector

were hydrogen-furnace-brazed to the manifold plate and the injector body with an 82% gold, 18% nickel-braze alloy.

(C) The face of the injector, with all 78 elements fastened interchangeably in place, is depicted in Fig. 5. The external mounting of deflectors in this experimental model was a matter of convenience. A flight version might utilize recessed deflectors (flush with the injector face) to minimize erosion when some of the elements are shut off during throttling (see Section V-C). The elements were oriented radially across the face, which was a spherical segment of 1-ft radius. All elements were therefore canted away from the chamber walls, with those in the outer ring canted the most (7 deg). Propellant momentum vectors in each spray were canted by a corresponding amount. Each element's impingement line was normal to a chamber radius and the fuel orifice of each pair was located on that side of the deflector closest to the center. Since there is some degree of penetration of the unlike sheets through each other at this level of thrust per element, (Ref. 10) the resultant spray fans were fuel-rich on the side closest to the chamber wall.

(C) The radial pattern was chosen for several reasons. First, orientation of the spray fans parallel to the wall aids in achieving a nearly uniform circumferential heat-transfer coefficient (Ref. 2) and minimizes local hot spots or "streaking" due to more direct impingement of oxidizer-rich spray fans on the wall. Second, fuel-rich sprays adjacent to the wall are capable of establishing an off-mixture-ratio or "barrier" zone, thereby lowering the effective driving temperature of the combustion gases and the overall level of chamber wall heat flux. This technique has resulted in remarkably low erosion rates for thrust chambers made of both ablative and pyrolytic graphite materials. In this particular case, no attempt was made to operate these outermost sprays at a lower than nominal mixture ratio.

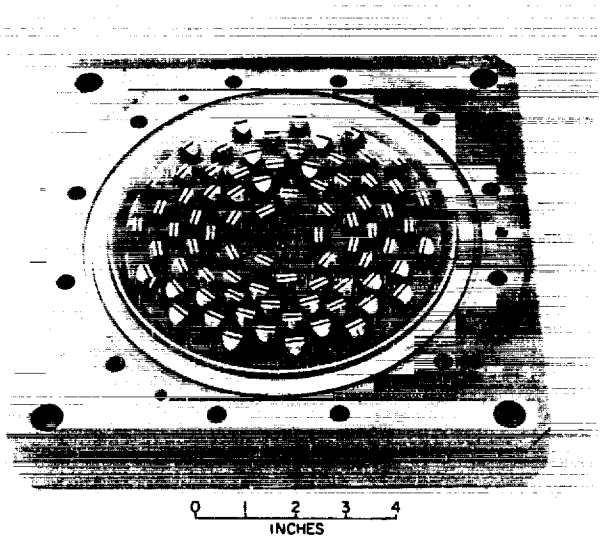

(C) Fig. 5. Face of 2000-lbf thrust, 78-element, impinging-sheet injector

(U) Ordinarily, a relatively uniform distribution of propellant mass flux across the face of an injector would seem desirable, since it would tend to minimize the nonaxial flow of combustion products from regions of high mass flux to those of lower mass flux. This flow could scour or erode the injector face. However, the use of a "hump-type" mass-flux distribution (which provides a maximum mass flux per unit area at the half radius of the injector and a minimum at the center and periphery) had been reported (Ref. 5) to be effective in minimizing coupling between the combustion process and the first tangential, first radial, and second tangential acoustic modes of instability. Accordingly, this type of programmed mass-flux distribution was adopted to help assure dynamic stability without the use of baffling. The additional face cooling, resulting from the use of the impinging-sheet elements, was expected to offset the deleterious effects of any "winds" that might result from the nonuniform mass distribution.

(U) The final pattern arrangement was obtained by laying out the spray fans of each individual element to provide the desired mass-flux distribution with optimum "close-packing" (minimum overlap and as few gaps as possible). This pattern is represented schematically in the artist's conception shown in Fig. 6. The mass-flux distribution measured across typical section A-A at full-thrust flow rates in nonreactive spray tests is shown in Fig. 7. Each of the 78 elements, which provided nominally 25.7 lbf of thrust at altitude, were used. An additional element might have been located at the geometric center of the injector face, but in the injector used in this study, that position was occupied by an auxiliary chamber pressure tap.

(U) Finally, it should be borne in mind that this injector was designed primarily as a constant-thrust device. Had it been designed specifically for pressure/area-step or discrete element throttling methods, some of the refinements suggested as a means of extending its throttle range could have been incorporated. See discussion of results (Section VI).

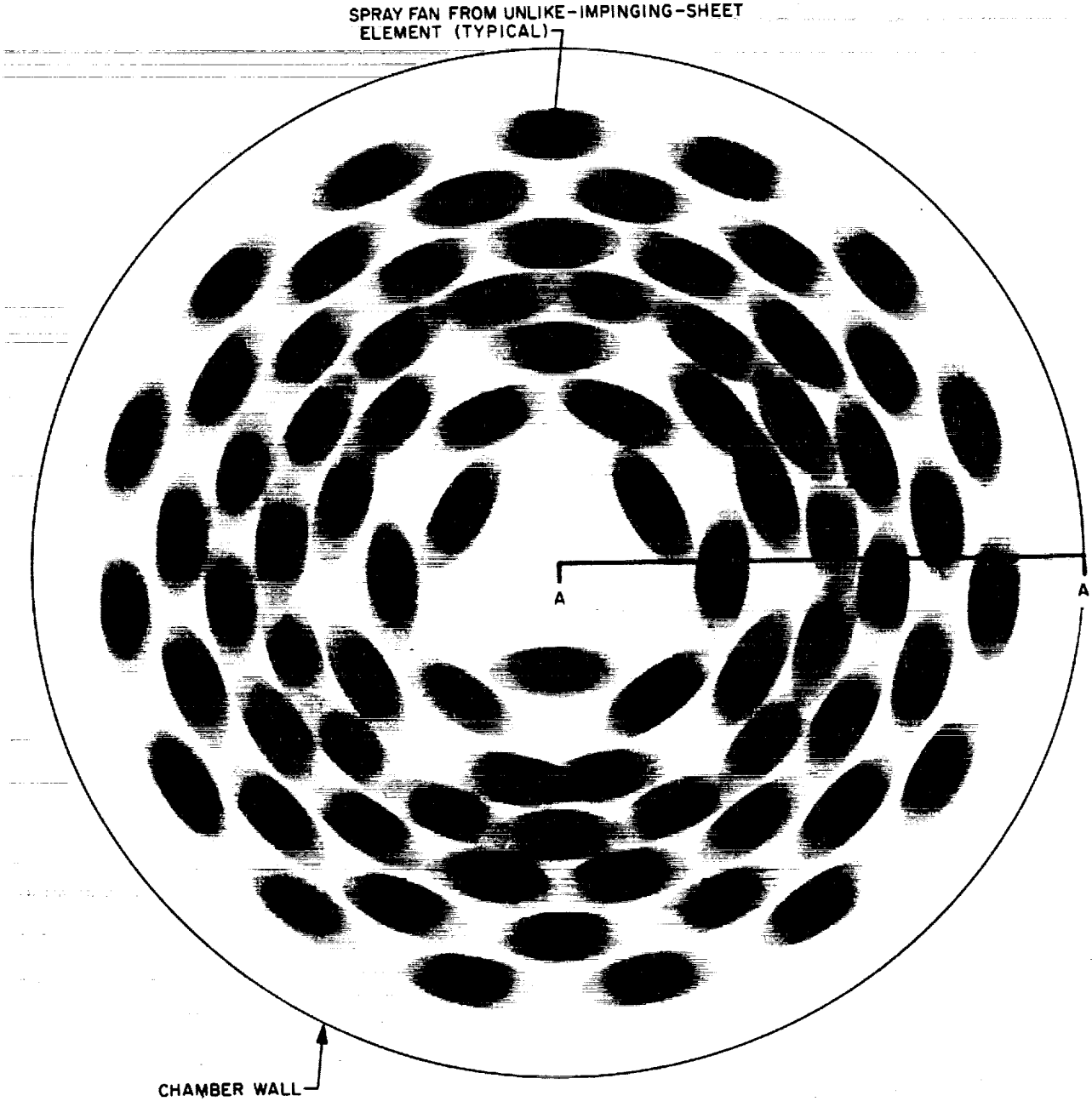

(C) Fig. 6. Mass distribution pattern near injector face at full thrust (looking toward injector), artist's conception

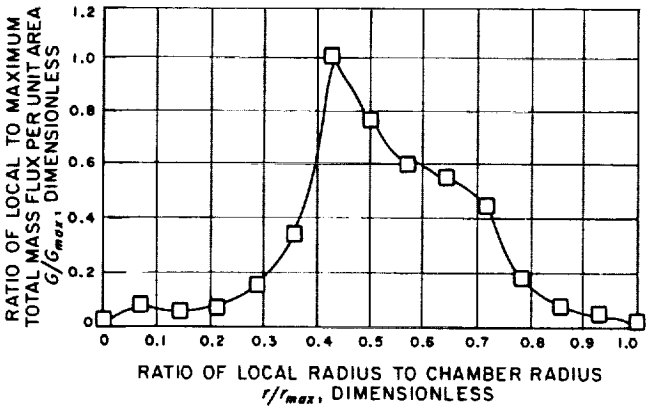

(U) Fig. 7. Average mass flux distribution for impinging-sheet injector through section A-A of Fig. 6

B. Thrust Chambers

(C) All firings were conducted in one of two uncooled, steel "work-horse" combustion chambers. The first, available from an earlier program, was instrumented with thermocouple plugs to permit heat-flux determinations by the method of Ref. 14, and during "sea-level" firings, with flush-mounted, high-frequency-response pressure transducers[2] to monitor combustion stability. Its geometry is summarized in Table 1. It was not feasible to install Photocons on those tests conducted in the vacuum chamber (see Section IV), but no instabilities were expected due to the very low chamber pressures in those tests. A second chamber, having the same nozzle geometry as the first, but built in spool-like sections so that its cylindrical length could be varied, was fabricated to determine the effect of chamber characteristic length on combustion efficiency (η_{c^*}). The additional characteristic lengths provided by this apparatus were 23.3 and 30.0 in. Unlike the 39-in.-L^* thrust chamber, however, the variable-L^* device was not instrumented with thermocouples for measuring nozzle and wall heat flux, or with Photocon transducers.

(C) Table 1. Thrust chamber geometry

Chamber parameters	Dimension
Throat area, A_t	7.67 in.^{2}
Contraction area ratio, ϵ_c	4.66
Expansion* area ratio, ϵ_e	2.43
Characteristic length, L^*	39.1 in.

*Optimum for expansion to atmospheric pressure at Edwards Test Station.

[2](U) Photocon Research Products, Pasadena, Calif.

III. Throttling Techniques

(U) In the absence of moving injector parts, the only throttling techniques deemed practicable were those which varied the total flowrate of combustible propellants (at constant throat area and supply pressure) by changing injection pressure, orifice area, or both. The momentum exchange concept and many of its proprietary or classified variations, which fall into this category and which might otherwise appear promising, are unfortunately linked with concentric stream or similar specific injector elements. The two throttling techniques selected because of their compatibility with unlike-impinging-sheet elements involved variation of injection pressure or flow area by devices external to the injector proper.

A. Pressure/Area-Step Method

(U) One technique, the pressure/area-step method, incorporates dual fuel and oxidizer manifolds. Dual-manifold throttling has been used in one form or another for a number of years (Refs. 15–19) and so is not an innovation in itself. In this concept, roughly half the total number of elements is fed from each manifold. At full thrust, both manifolds (all of the injection elements) are used. Thrust reduction is accomplished by pressure-throttling the full flow area (all manifolds) until injection pressure drops have decreased almost to the point of incipient low-frequency instability (feed-system interaction). The chamber pressure will meanwhile have correspondingly decreased. Then one pair of manifolds (fuel and oxidizer) is completely valved off, so that the propellants flow through only about half the original injector orifice area. This increases injection pressure drops by a factor of about four, which is compatible with the constant supply pressure and reduced chamber pressure. Further thrust reduction results from pressure-throttling the remaining orifice area. One advantage of this technique is that, since about half the elements remain "on" during throttling, it is possible to maintain a programmed mass flux and mixture ratio distribution across the face of the injector, even under deep-throttled conditions. This facilitates the prediction and control of combustion stability, as well as chamber and nozzle heat-transfer characteristics. Another advantage is the relatively simple external manifolding, valving, and plumbing required. However, the large liquid volume of the dual manifolds could introduce hydraulic lag, and any propellants trapped in them at shutoff might thermally decompose.

B. Discrete-Element Method

(U) The second throttling technique studied, the discrete-element method, uses no propellant manifolds per se. Instead, each individual fuel orifice is connected directly to a fuel throttle valve by means of its own feeder tube. The valve is constructed in such a way that it can shut off discrete fuel orifices one at a time (or several at a time, if desired). Similarly, each oxidizer orifice is fed directly by an oxidizer throttle valve. The valves are mechanically linked and the combination driven by a single actuator. Throttling is accomplished as the valve progressively opens (or closes) the entrances to the individual feeder tubes, thus turning on (or shutting off) discrete injection elements singly or in groups. Each element can be full on, full off, or partially open, permitting a fine degree of throttling. If supply pressure were held constant, injection pressure drops would *increase* as flowrates were reduced by the change in total orifice area of the injection element.

(C) The successful implementation of this concept requires the use of an injection element that is inherently so efficient that secondary interactions between its own spray and the sprays produced by its neighbors are not as necessary for efficient propellant mixing and combustion. Only in this way can performance degradation be avoided under deep-throttled conditions, when a few relatively isolated elements remain on. One such element is JPL's unlike-impinging-sheet device. The work of Ref. 11 showed that single impinging-sheet elements could deliver c^* efficiencies in excess of 95% over a wide range of injection velocities with the N_2O_4/N_2H_4 propellant combination. A second requirement is the availability of a suitable valve that can perform the discrete-orifice throttling. Such a valve, incorporating both the on-off and throttling functions and being developed at JPL, has proven feasible. Its design, fabrication, and hydraulic characteristics are described in Ref. 20.

C. Fixed-Point Simulation of Throttling Techniques

(U) To reduce costs, continuous throttling was not employed in this program. Instead, fixed-point tests were conducted, in which the steady-state total propellant flowrate remained constant during each individual test, but varied from one test to the next. Instead of using a set of dual manifolds for pressure/area-step throttling, or multiport throttle valves for discrete-element throttling, flow area changes were effected by inserting Teflon plugs in the manifold plate (Fig. 4) to close off the entrances to the desired feeder tubes.

IV. Test Conditions

(U) The experimental effort was conducted in three series of test firings at the Edwards Test Station facility operated by JPL for NASA. The first two series placed primary emphasis on evaluation of the two throttling techniques discussed in Section III. Both were conducted with N_2O_4/N_2H_4 propellants at a nominally constant mixture ratio of 1.2 in the 39-in.-L^* (characteristic-length) thrust chamber (Table 1). The third series was designed to determine the effects on combustion efficiency of using other, chemically similar propellant combinations, and of excursions in mixture ratio and chamber characteristic length. In all three series, the firings were of short duration (1–8 s).

(C) In the first series, 18 firings were made with N_2O_4/N_2H_4 propellants to evaluate the combustion efficiency (η_{c^*}) and heat transfer (h_g) characteristics of the 78-element impinging-sheet injector in the pressure/area-step throttle mode. First, the full flow area, with a mass distribution pattern similar to that represented in Fig. 6, was throttled from a total flowrate of 6.54 to 2.33 lbm/s by reducing the injection pressure. The chamber pressure ranged from 152 to 46 psia. Next, 33 elements were shut off by plugging their feeder tubes to simulate valving off one pair of propellant manifolds. The mass distribution pattern of the remaining 45 elements is shown schematically in Fig. 8. Although the total orifice flow area was reduced by 42%, this spray-fan arrangement preserved the "hump-type" mass-flux distribution considered desirable from stability considerations. At this constant and reduced flow area, the injector was further pressure-throttled from a total flowrate of 3.99 to 1.66 lbm/s. The chamber pressure varied correspondingly from 93 to 30 psia. It was recognized, however, that such a relatively nonuniform distribution might not promote optimum secondary mixing, and therefore not yield maximum performance efficiencies at the lower thrust levels. So the reduced-area portion of this simulated throttle cycle was repeated with 36 elements shut off.

(C) The mass distribution pattern for the remaining 42 elements is illustrated in Fig. 9. Since the distribution of propellants across the face of the injector was more nearly uniform with this pattern, it was expected that performance (η_{c^*}) levels would be generally higher than those obtained with the pattern of Fig. 8. At this constant, reduced flow area, the injector was pressure-throttled from a total flowrate of 3.96 to 1.58 lbm/s. The chamber pressure varied from 92 to 31 psia. The lower limit of chamber

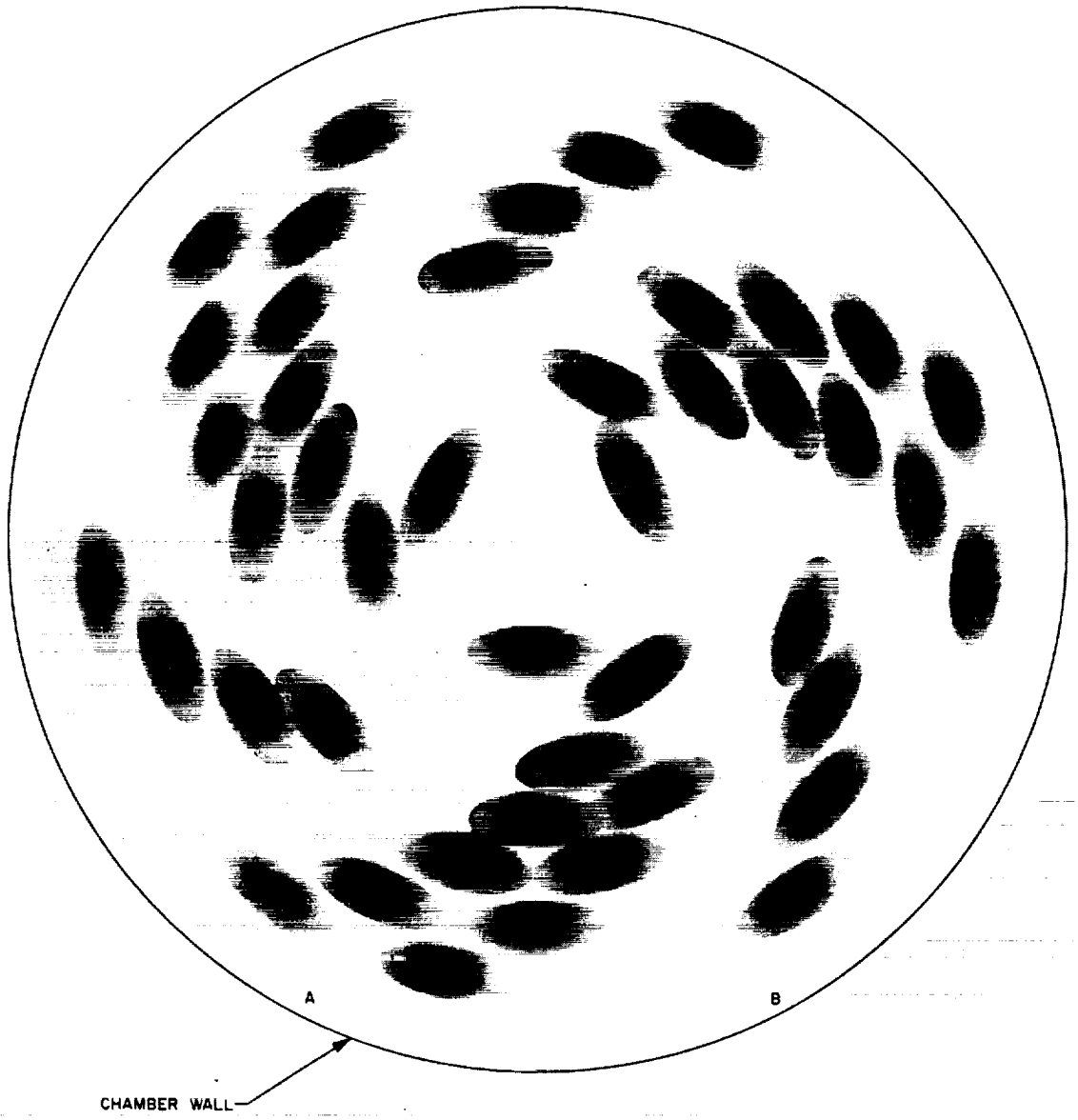

(C) Fig. 8. Mass distribution pattern near injector face with 33 elements shut off (looking toward injector), artist's conception

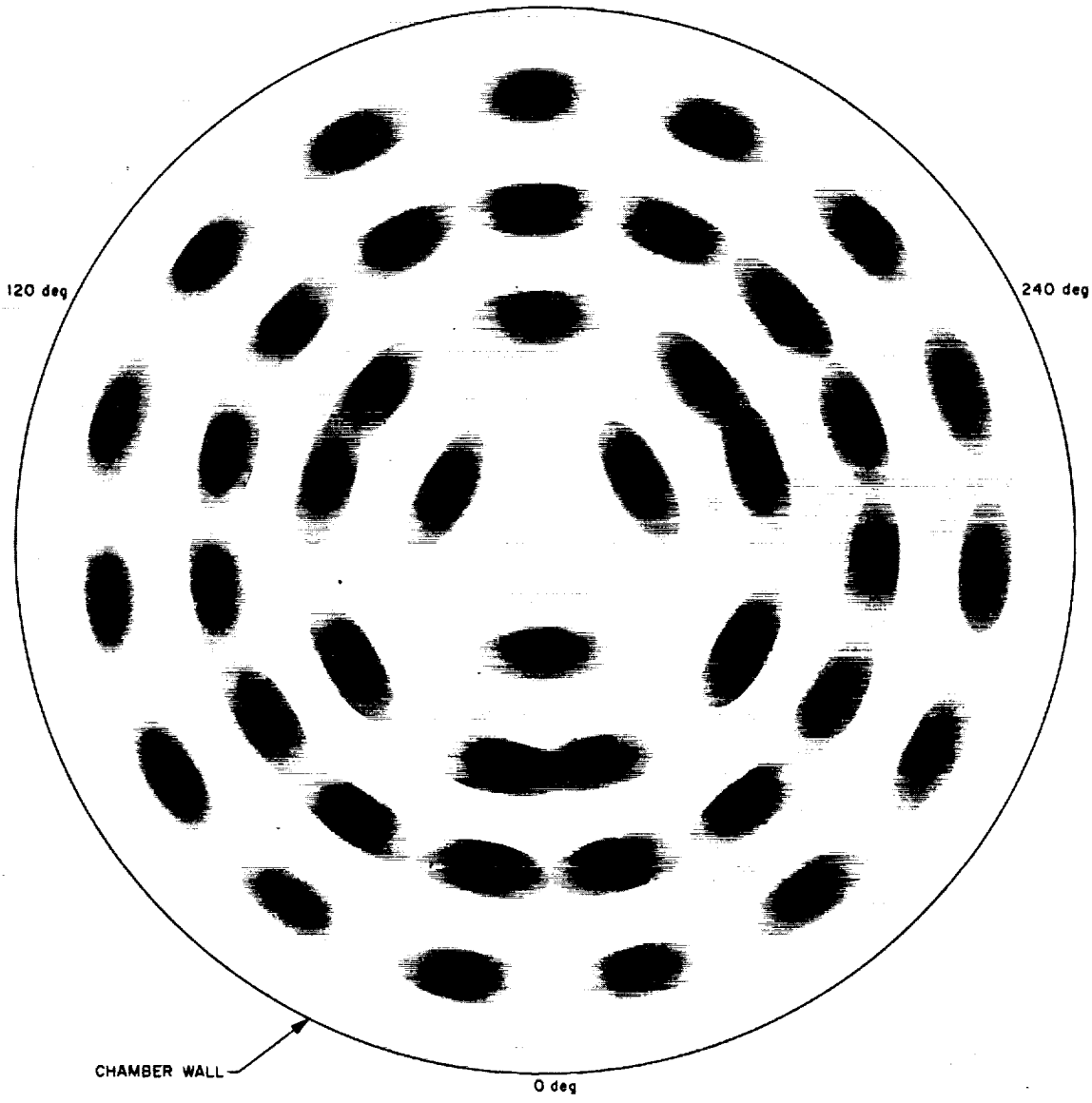

(C) Fig. 9. Mass distribution pattern near injector face with 36 elements shut off (looking toward injector), artist's conception

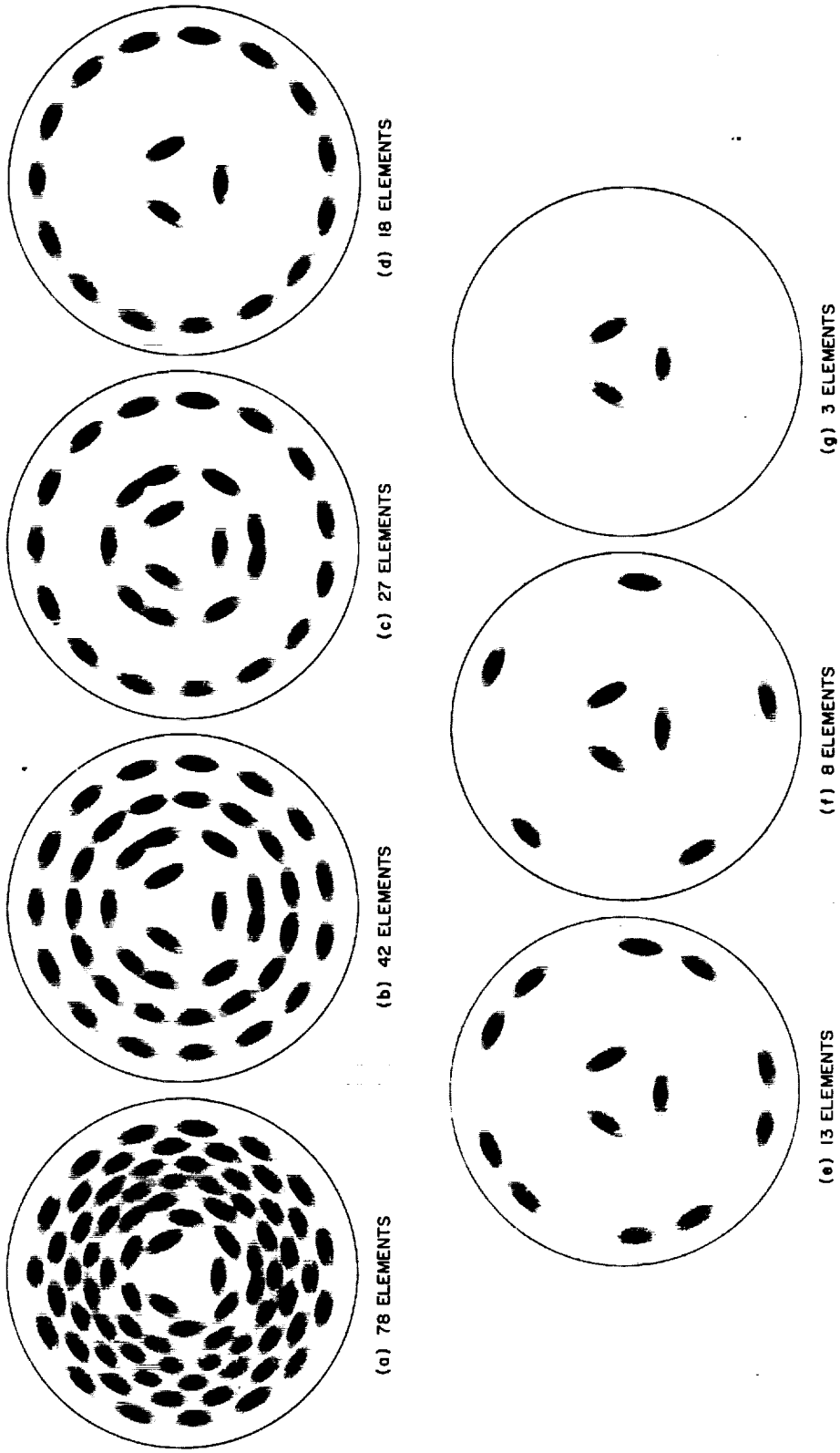

(C) Fig. 10. Discrete-element throttling, showing mass distribution patterns near injector face with various numbers of elements firing, artist's conception

pressure (30 psia) in this first series of firings was sufficiently high that all firings could be conducted at ground level ($P_a \cong 13.5$ psia).

(U) In the second series, 13 N_2O_4/N_2H_4 firings were made to evaluate the performance delivered by the impinging-sheet injector when throttled by the discrete-element technique. By inserting Teflon plugs to close off the entrances to various orifice feeder tubes, injector patterns consisting of 27, 18, 13, 8 and 3 elements were obtained. These are shown in Fig. 10 (c) through (g). Several firings were made with each pattern to assess the effects of varying chamber pressure and injection velocity on η_{c^*}. From the data obtained in this series of firings, as well as that collected in the first series with element configurations 10 (a) and (b), it was later possible to synthesize curves of the key performance parameters vs the throttle ratio. Approximately half the firings were conducted at the test station ambient pressure (13.5 psia). The remainder (those at chamber pressures below about 30 psia) were made in the Edwards Test Station altitude chamber to assure that the nozzle ($\epsilon = 2.43$) would flow sonic without separation during deep-throttled firings.

(U) To minimize the possibility of ignition overpressures, or "spiking," the simulated altitude firings were started at an intermediate pressure level (about 3–4 psia). Upon ignition, the vacuum chamber was quickly exhausted to the "altitude" conditions (0.1–0.5 psia, depending on engine flow rate) under which the steady-state data were recorded. However, this technique was only a convenient "fix" to facilitate smooth starts in this series of experiments. When started under hard vacuum, the engine exhibited the high transient overpressures ("spikes") typical of altitude ignition with this class of propellants. All the N_2O_4/N_2H_4 firings in these first two test series were conducted with the original steel deflectors.

(C) As a part of a broader program to evaluate maximum-density fuming nitric acid (MDFA) as a candidate oxidizer for the *Voyager* lander, a third series of 25 test-firings was conducted using MDFA with two different candidate fuels: hydrazine (N_2H_4) and monomethylhydrazine (MMH). MDFA is a mixture of 56% HNO_3 and 44% N_2O_4 by weight. Its physical properties are summarized in Ref. 21. This propellant shows some promise as an oxidizer for future spacecraft applications because, compared to other earth-storable oxidizers, such as N_2O_4, it has a lower vapor pressure and a higher density at the elevated temperatures required by the planetary quarantine thermal sterilization. All 78 elements remained flowing in each test of this series. Excursions were made in chamber pressure ($75 < P_c < 150$) and mixture ratio ($1.0 < r < 1.8$). The MDFA/N_2H_4 firings were all made at a constant chamber characteristic length of 39 in., but the MDFA/MMH firings were conducted at L^*'s of 23.3, 30, and 39 in. Since deep throttling was not attempted, all firings were made at test station ambient pressure. For the MDFA test firings, the injector was refurbished with a new complement of molybdenum deflectors.

V. Experimental Results

A. Performance

(C) The performance results are summarized in Tables 2–5. Table 2 presents the results of the first series of firings, for which pressure/area-step throttling was simulated, whereas Table 3 exhibits performance data for the second series, in which discrete-element throttling was simulated. Tables 4 and 5 summarize the results of the third test series, designed to study the effects of changes in propellant combination, chamber characteristic length, and propellant mixture ratio. For convenience, the results are reported in two separate tables, one for the MDFA/N_2H_4 propellants (Table 4), and another for MDFA/MMH (Table 5).

(C) The durations reported are steady-state values. The use of the uncooled thrust chamber and the low-conductivity steel deflectors made short firing durations mandatory. The chamber pressures reported are stagnation values obtained from static measurements made near the entrance to the converging portion of the nozzle by applying the standard static-to-stagnation correction. These agreed within ±0.5% with corrected chamber pressure values obtained from the pressure tap in the injector face. The reported values of c^* are based on the calculated stagnation pressures, but no other corrections have been made to c^*. When extant methods of correcting for heat loss, throat area change and radius of curvature, nozzle discharge coefficient, and frictional drag losses were applied to the data to obtain an estimate of the total correction to c^*, they combined in such a way as to introduce only negligible changes in the reported values. The tabulated values of η_{c^*} are included mainly for comparative purposes. They were calculated by taking the ratio of the uncorrected measured values to the theoretical full-shifting equilibrium values at the experimental chamber pressures and mixture ratios.

(C) Table 2. Results of N_2O_4/N_2H_4 firings simulating pressure/area-step throttling, test series 1

Test No.	No. of elements firing	Duration, s	Oxidizer/fuel mixture ratio, r	Chamber pressure P_c, psia	Total flow-rate $\dot{w}_t$, lbm/s	Thrust F, lbf	Characteristic velocity c*, ft/s	Characteristic velocity efficiency η_{c^*}, %	Combustion roughness parameter $\frac{\Delta P_c}{P_c}$, %
1	78	1.6	1.26	152.3	6.54	1441	5720	98.5	1.3
2	78	1.6	1.22	149.1	6.39	1368	5724	98.5	[a]
3	78	2.1	1.21	135.2	5.80	1271	5723	98.5	[a]
4	78	1.6	1.22	123.1	5.33	1113	5662	97.6	1.3
5	78	1.8	1.21	112.2	4.84	996.2	5698	98.2	[a]
6	78	1.8	1.25	98.87	4.27	845.8	5683	98.4	3.0
7	78	2.0	1.25	89.03	3.85	733.2	5686	98.4	[a]
8	78	1.9	1.43	78.63	3.47	614.3	5572	98.3	2.5
9	78	3.2	1.21	46.12	2.33	332.0	4900	83.0	[a]
10	45	2.1	1.14	92.85	3.99	782.6	5709	98.3	1.7
11	45	1.8	1.20	69.15	3.04	517.5	5594	96.7	1.4
12	45	2.6	1.26	45.31	2.12	304.4	5247	91.4	2.0
13	45	3.0	1.18	30.22	1.66	178.2	4465	77.7	1.7
14	42	2.5	1.17	92.23	3.96	777.4	5729	98.7	1.3
15	42	2.9	1.18	78.37	3.39	633.9	5682	98.1	[a]
16	42	2.4	1.20	69.73	3.03	526.5	5649	97.6	1.3
17	42	2.6	1.15	46.44	2.04	441.4	5600	96.9	1.7
18	42	2.7	1.10	30.72	1.58	189.6	4782	83.5	1.0

[a]No reading obtained, due to transducer malfunction.

(C) Table 3. Results of N_2O_4/N_2H_4 firings simulating discrete-element throttling, test series 2

Test No.	No. of elements firing	Duration, s	Oxidizer/fuel mixture ratio, r	Chamber pressure p_c, psia	Oxidizer injection pressure drop, psid	Total flow-rate, $\dot{w}_t$, lbm/s	Thrust F, lbf	Characteristic velocity c*, ft/s	Characteristic velocity efficiency η_{c^*}, %
19	27	3.5	1.19	83	170	3.61	698	5660	97.7
20	27	3.5	1.19	67	111	2.90	528	5670	98.0
21	27	2.5	1.22	49	68	2.21	345	5490	95.3
22	27	2.5	1.22	47	64	2.15	331	5420	94.2
23	27	4.0	1.16	39	41	1.74	268	5550	96.3
24	18	3.0	1.20	56	164	2.45	390	5600	97.0
25	18	4.0	1.12	32	57	1.37	—[a]	5660	98.0
26	13	3.0	1.19	40	177	1.79	301	5500	96.3
27	13	4.5	1.17	24	64	1.09	—[a]	5500	95.7
28	8	5.0	1.13	25	195	1.13	—[a]	5510	96.0
29	8	5.5	1.14	15	66	0.691	—[a]	5416	94.4
30	3	6.5	1.24	9	211	0.455	—[a]	4831	—[b]
31	3	8.0	2.24	4	74	0.2	—[a]	4914	—[b]

[a]Not measured; altitude cell thrust mount not available at Edwards Test Station.

[b]Reliable theoretical performance data not available.

(C) Table 4. Results of MDFA/N_2H_4 firings (characteristic length of chamber $L^* = 39$ in.), test series 3

Test No.	Duration, s	Total flowrate $\dot{w}_t$, lbm/s	Oxidizer/fuel mixture ratio, r	Chamber pressure P_c, psia	Thrust F, lbf	Pressure drops, psid		Fuel injection velocity, ft/s	$\mathcal{R}$ (Eq. 4)	Characteristic velocity c^*, ft/s	Characteristic velocity efficiency η_{c^*}, %
						Oxidizer	Fuel				
32	1.5	6.90	1.20	156	1473	56	64	82.0	0.47	5570	96.1
33	1.6	6.59	1.27	159	1395	54	54	75.7	0.50	5570	96.4
34	2.0	6.64	0.96	150	1390	47	71	88.4	0.36	5550	95.8
35	1.9	6.97	1.72	151	1402	125	41	66.8	0.65	5320	95.7
36	2.1	4.56	1.23	102	856	28	26	53.2	0.49	5510	95.3
37	2.4	4.66	1.70	100	843	38	19	44.9	0.64	5285	95.1
38	2.4	4.45	0.98	101	570	22	32	58.7	0.37	5550	95.9
39	3.0	3.40	1.19	77	581	16	16	40.5	0.47	5530	95.6
40	3.0	3.53	1.72	76	566	24	12	33.9	0.65	5280	95.5
41	3.0	3.36	0.93	75	588	14	20	45.4	0.35	5780	95.4

(C) Table 5. Results of MDFA/MMH firings, test series 3

Test No.	Duration, s	Total flowrate $\dot{w}_t$, lbm/s	Oxidizer/fuel mixture ratio, r	Chamber pressure P_c, psia	Thrust F, lbf	Chamber characteristic length L^*, in.	Pressure drops, psid		Fuel injection velocity, ft/s	$\mathcal{R}$ (Eq. 4)	Characteristic velocity c^*, ft/s	Characteristic velocity efficiency η_{c^*}, %
							Oxidizer	Fuel				
42	3.0	6.68	1.19	143	1319	39.1	57	70	92.1	0.43	5250	96.0
43	3.1	7.03	1.39	154	1444	39.1	72	65	88.5	0.51	5370	96.1
44	3.5	4.62	1.22	98	834	39.1	31	32	62.6	0.45	5220	95.1
45	3.6	6.95	1.34	151	1420	30.0	63	69	89.4	0.49	5320	96.0
46	3.3	4.67	1.38	101	863	30.0	28	34	59.0	0.51	5315	95.6
47	3.2	3.61	1.42	78	605	30.0	17	22	44.7	0.52	5310	95.4
48	3.1	6.91	1.40	152	1420	23.3	70	61	86.5	0.51	5390	96.8
49	3.1	7.16	1.01	147	1362	23.3	58	91	107.0	0.36	5300	94.7
50	3.2	6.88	1.77	152	1428	23.3	84	44	74.8	0.63	5420	96.2
51	3.6	4.65	1.28	101	846	23.3	32	29	61.1	0.47	5300	96.2
52	4.1	4.98	0.98	102	863	23.3	30	43	75.5	0.34	5000	94.9
53	4.1	4.65	1.75	102	876	23.3	41	20	50.9	0.62	5390	96.2
54	4.6	3.50	1.30	75	573	23.3	20	17	45.8	0.48	5290	95.8
55	4.6	3.76	1.02	77	597	23.3	19	24	56.1	0.36	5040	94.9
56	4.6	3.43	1.72	75	570	23.3	24	12	37.8	0.62	5350	95.6

(U) The values of thrust reported are those measured in the firings conducted at ambient pressure (approximately 13.5 psia) with an expansion area ratio of 2.43. Superscript —* in Table 3 indicates firings made with the same thrust chamber in the Edwards Test Station altitude facility. Because a thrust mount suitable for use with the present engine assembly and compatible with the vacuum chamber was not available during testing, thrust could not be measured for the altitude firings.

(C) The chamber pressure in the two 3-element firings (Tests 30 and 31 of Table 3) was below the vapor pressure of nitrogen tetroxide at injection conditions. The low values of c^* for these two firings are attributed to the oxidizer flashing, which, under these circumstances, would be expected and would adversely affect the degrees of propellant mixing and atomization attainable. Therefore, it is felt that the results of Tests 30 and 31 cannot properly be compared with those of the other firings on an equal basis. In the discussion of results (Section VI), no further consideration will be given the 3-element firings.

B. Heat Transfer

(U) Although not a primary objective of this program, chamber and nozzle wall-heat-flux measurements were made for a limited number of firings during the first test series (pressure/area-step performance evaluation). The chief difficulty encountered in obtaining this information was the combination of short firing durations (necessary to preserve the steel chamber) and low chamber pressures during throttling. Because of these, the thrust chamber walls and throat did not reach temperatures in excess of 300°F and 800°F, respectively, in the second series of firings (discrete-element throttling). In most cases, the maximum temperatures were even lower. This limited thermal response was not sufficient to permit accurate calculation of local heat-flux and gas-side film coefficients. Heat-transfer measurements were not made in the third test series, since the variable-L^* chamber used was not thermally instrumented.

(U) Table 6 summarizes the heat-transfer results of those tests within the first series for which sufficiently good data was obtained. The test numbers correspond to those in Table 2. The heat-flux values were calculated by a computer program based on the method of Ref. 14. Values of q/A and h_g in the chamber are referenced to an inside wall temperature of 500°F, since, in these short-duration firings, the inside chamber walls did not attain the 1000°F customarily used as the reference condition. The driving-gas (stagnation) temperature T_o was estimated from the theoretical combustion temperature T_c by means of the familiar relationship

$$T_o = T_c\,(\eta_{c^*})^2 \tag{1}$$

which assumes the boundary and core flow properties are identical, and where the T's are absolute values. Gas-side heat-transfer coefficients then followed from

$$h_g = \frac{q/A}{T_o - T_w} \tag{2}$$

(U) Table 6. Summary of heat-transfer results, test series 1

Test No.	No. of elements firing	T_o, °F	Chamber[b]		Nozzle throat	
			$q/A_{500°F}$, $\frac{\text{Btu}}{\text{in.}^2/\text{s}}$	$h_{g500°F}$, $\frac{\text{Btu}}{\text{in.}^2/\text{s}/°\text{F}} \times 10^{-4}$	$q/A_{1000°F}$, $\frac{\text{Btu}}{\text{in.}^2/\text{s}}$	$h_{g1000°F}$, $\frac{\text{Btu}}{\text{in.}^2/\text{s}/°\text{F}} \times 10^{-4}$
1	78	4959	2.68	6.0	7.32	18.5
2	78	4909	2.65	6.0	7.23	18.5
3	78	4876	2.21	5.04	6.97	18.0
4	78	4772	1.96	4.59	6.22	16.5
5	78	4817	1.76	4.08	5.84	15.3
6	78	4832	1.56	3.6	4.79	12.5
7	78	4817	1.37	3.17	4.01	10.5
8*	78	4906	1.17	2.65	3.36	8.6
10*	45	4777	1.48	3.46	5.29	14.0

*Tests 9 and 11–13 were not of long enough duration to permit accurate calculation of heat flux values.
[b]Average of nine measurements.

(U) In Table 6, "chamber" refers to an axial station in the cylindrical portion of the thrust chamber, approximately 5 in. downstream of the injector face. At that station, nine separate thermocouples, equally spaced around ⅓ of the chamber circumference, permitted a determination of the degree to which h_g varied around the chamber. The values of q/A and h_g presented in Table 6 under "chamber" are averages of the nine individual readings. The average deviations were negligible.

C. Durability of Injection Elements

(U) During the first series of tests (Table 2) it was noted that, in Tests No. 1 through 9, some minor localized burning or erosion had occurred on the sides of some of the steel deflectors. This had been expected with steel, due to its relatively low thermal conductivity. However, aside from some discoloration, none of the actual sheet-formation surfaces was damaged, and the same deflectors continued to be used throughout the pressure/area-step throttling tests. The durability of these deflectors is attributed to the cooling effects of the propellant sheets flowing on them.

(U) On the other hand, beginning with Test No. 10 of Table 2, all the deflectors that had been totally shut off to effect the reduction in flow area were severely burned and most were rendered unserviceable. This is evident from Fig. 11, in which the post-test appearance of

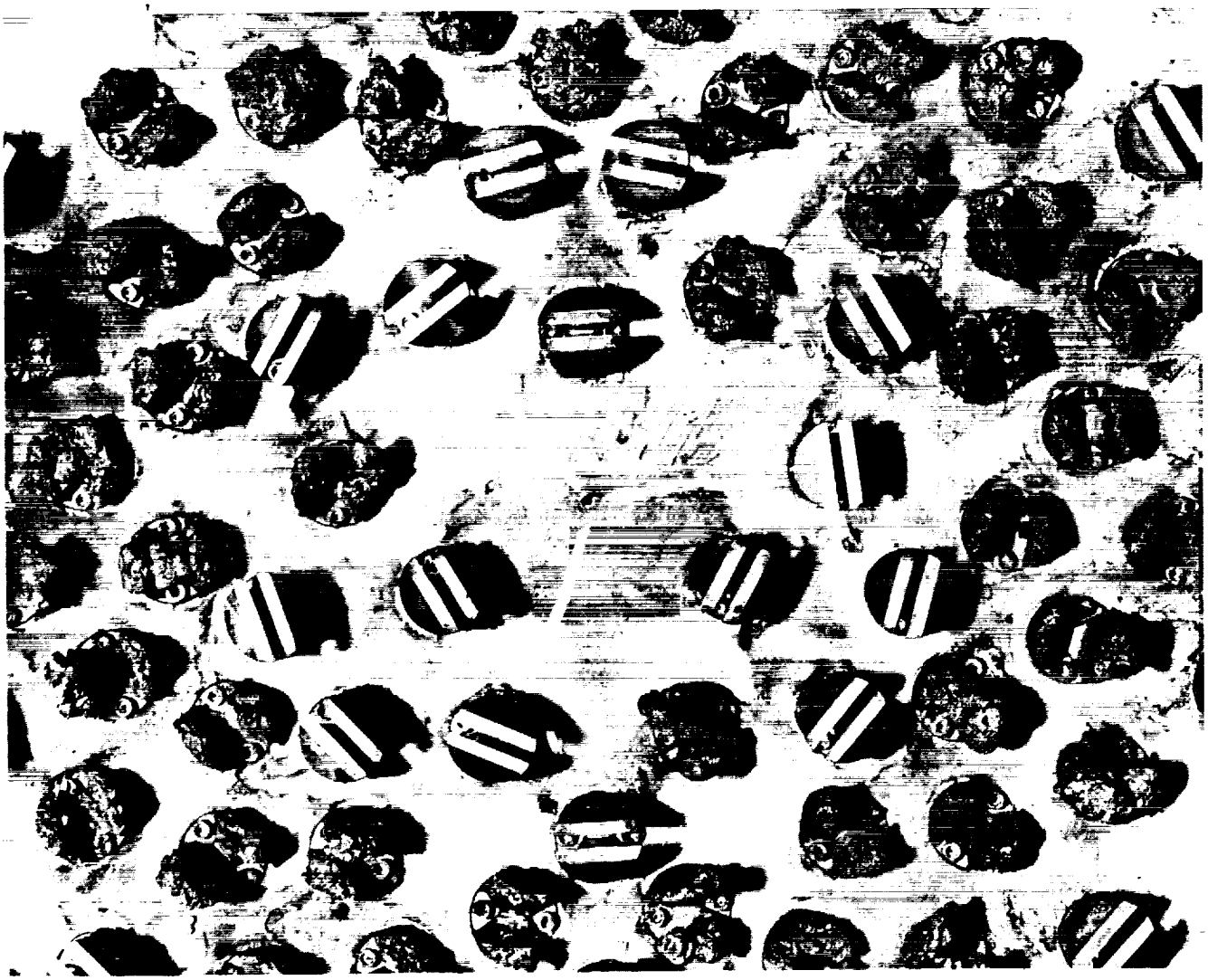

(C) Fig. 11. Post-test appearance of cooled and uncooled steel deflectors

propellant-cooled deflectors, and those which had been shut off, may be compared. To conserve deflectors in test series 2 (Table 3), the shutoff elements were removed and replaced with sheet metal discs.

(U) Between test series 2 and 3, the injector was refurbished with a new complement of elements, so that all the maximum-density acid firings were conducted with the electrodischarge-machined TZM molybdenum deflectors. Since no elements were turned off in the MDFA firings, no erosion or burning of the molybdenum deflectors was found, and all elements remained serviceable after the 25 firings of Tables 4 and 5. Subsequent to Test No. 56, three additional firings were attempted, once again with N_2O_4/N_2H_4, but in each case a "hard start" was encountered (chamber pressure peaked at around 350 psia), which destroyed a number of elements. The exact cause of the pressure spikes was not determined, but sufficient numbers of elements were damaged to terminate the experimental program. Figure 12 shows the post-test appearance of the injector after one of the hard starts. Four elements have been completely sheared

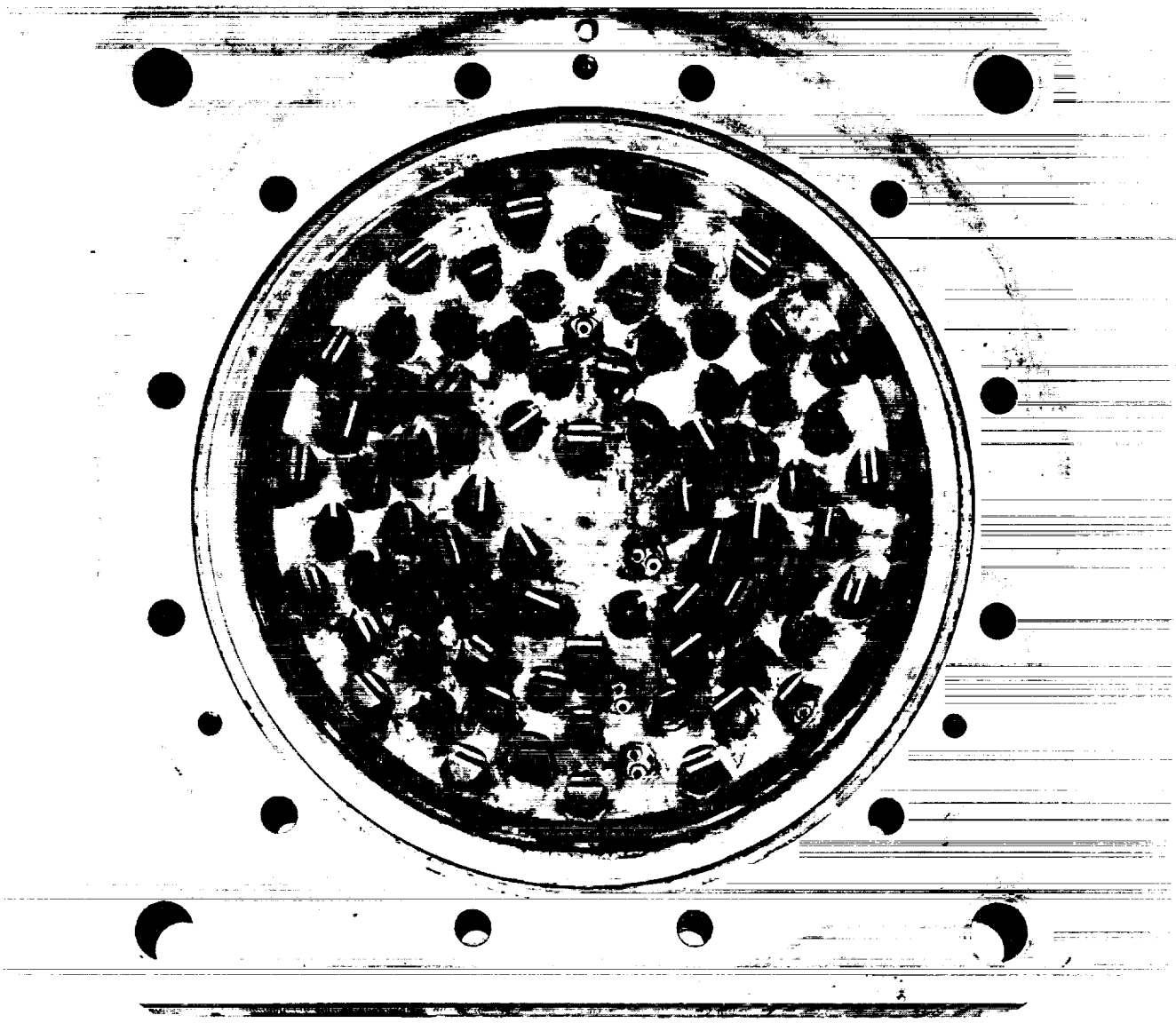

(C) Fig. 12. Post-test appearance of injector after "hard start" with molybdenum deflectors

off and one (in the lower right corner) has lost one deflector.

D. Combustion Stability and Smoothness

(U) There was no evidence of high-frequency combustion instability arising spontaneously in any of the 56 firings made during this program. In the additional tests planned, the chamber was to be bombed to assess dynamic stability, but destruction of a large portion of the molybdenum deflectors, as described above, precluded that effort.

(C) The parameter $\Delta P_c/P_c$ is presented in Table 2 as a measure of combustion roughness. ΔP_c is the root-mean-square amplitude of high-frequency chamber pressure oscillations. Similar results, indicating relatively noise-free combustion, were obtained in the remaining firings, as well. In no case did $\Delta P_c/P_c$ exceed 3%, and in most instances the values ranged between 1 and 2%. For the sake of brevity, $\Delta P_c/P_c$ has not been reported in Tables 3–5. No "pops" were noted, either.

VI. Discussion of Results

A. Performance During Simulated Pressure/Area-Step Throttling

(U) Characteristic velocity efficiency, chamber pressure, and injection pressure drop are plotted vs a throttle ratio ϕ (Figs. 13–15) for the N_2O_4/N_2H_4 pressure/area-step throttled firings of Table 2. These figures represent only the 78- and 42-element pattern arrangements, since the relatively nonuniform 45-element pattern of Fig. 8 gave a somewhat lower c^* efficiency (Test Nos. 10–13, Table 2) than the more uniform arrangement of Fig. 9 did. This was probably due to less complete secondary propellant mixing and provided a less uniform circumferential heat-flux distribution. For these reasons, it was felt that the 42-element configuration was a more reasonable choice for use in area step-change throttling, and all subsequent discussions will be based on it. However, the 42-element arrangement of Fig. 9 is still not necessarily the optimum one, and the selection of an alternate one might yield somewhat increased performance during throttling. For the sake of brevity, Fig. 15 shows only the oxidizer injection pressure drop, but it will be recalled that the fuel and oxidizer pressure drops were nominally the same, both by design and in actual fact.

(C) The throttle ratio ϕ is defined as the total weight flowrate ($\dot{w}_t$) at maximum thrust (in this case, 6.54 lbm/s for an altitude thrust of 2000 lbf at an expansion area

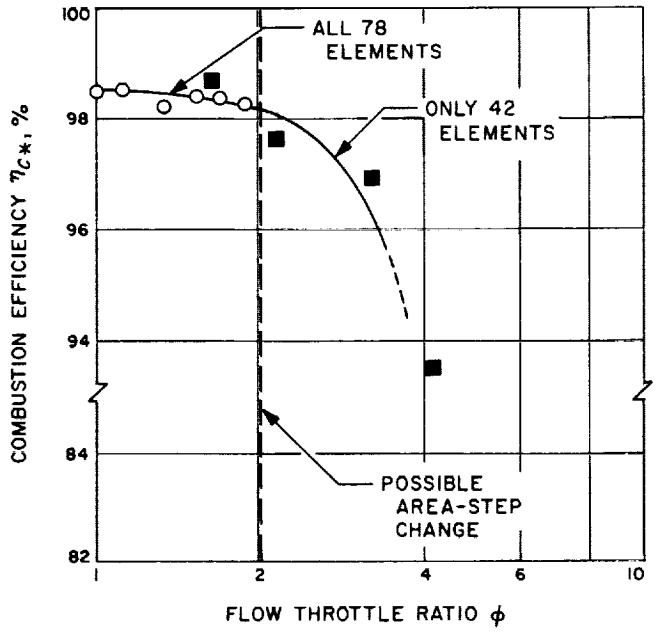

(C) **Fig. 13. Variation of c^* efficiency during pressure/area-step throttling**

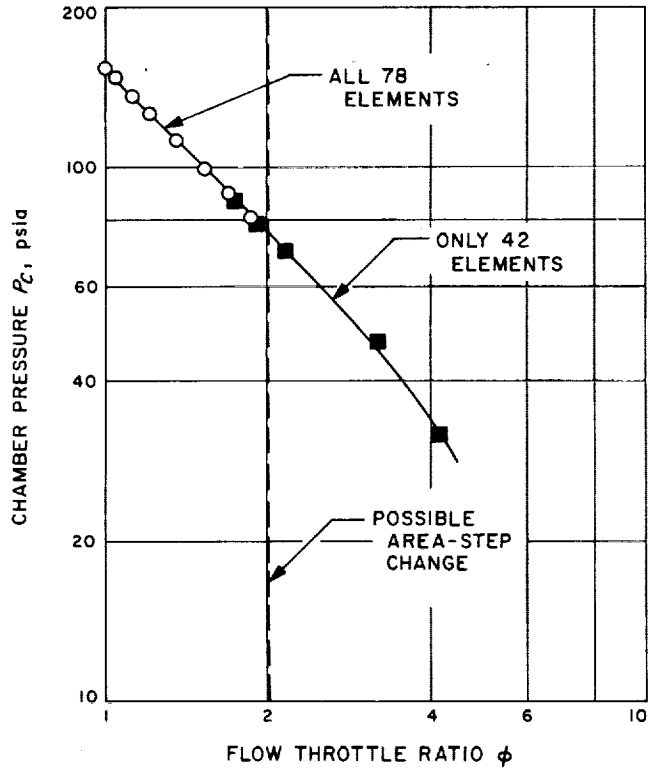

(U) **Fig. 14. Variation of chamber pressure during pressure/area-step throttling**

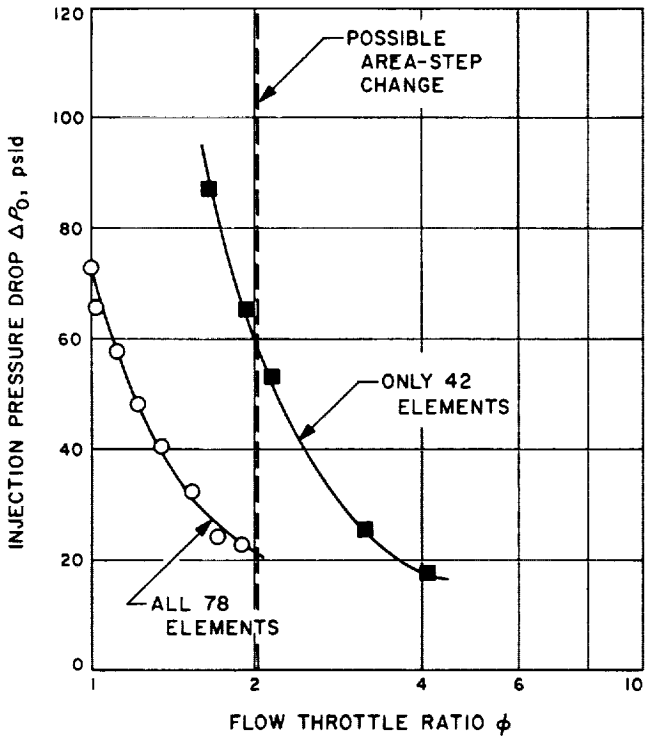

(U) Fig. 15. Variation of injection pressure drop (fuel or oxidizer) during pressure/area-step throttling

ratio of 40:1) divided by the total weight flowrate measured in a particular test. This ratio is numerically very close to the corresponding ratio of maximum altitude thrust (2000 lbf) to the altitude thrust calculated for each test from the relationship

$$F = C_F P_c A_t \tag{3}$$

taking C_F constant at the calculated value of 1.75 ($\epsilon_e = 40{:}1$). In this report, however, ϕ has been defined in terms of weight flows, so that the throttle ratios can be derived from actually measured, rather than calculated, values.

(C) Figures 13–15 illustrate how the key combustion parameters would be expected to vary during continuous throttling by the pressure/area-step method. For example, the variation of c^* efficiency with throttle ratio is plotted in Fig. 13. The combustion efficiencies, measured during the reduction of propellant flow to all 78 elements (by throttling the manifold supply pressure), are shown in Fig. 13 as open circles. The black data points represent those tests in which similar pressure throttling was applied to the reduced flow area comprising only 42 elements. Note that c^* efficiency dropped below the desirable minimum value of 95% (as called for by the program objectives) after throttling over a range of about 3.75 to 1. A throttle ratio of 2 is indicated on Fig. 13 as one possible point at which the area step-change could be made, since (see Fig. 15) the pressure drop across all 78 elements decreased to only about 20 psid at that point. The decrease in c^* efficiency at throttle ratios greater than about 3 was quite rapid. This decrease in efficiency is attributed to a decline in the combustion efficiency of each individual element, probably due to a degradation in propellant mixing and atomization, as injection velocities were reduced.

(U) The variations in chamber pressure and injection pressure drop are shown in Figs. 14 and 15, respectively. Here, there is a continuous and nearly linear variation in chamber pressure across the transition from the 78- to the 42-element flow area. The pressure drop (Fig. 15) initially declines (very nearly as ϕ^{-2}) during throttling of the full-flow area, then increases suddenly as the flow area is reduced at constant ϕ, and then declines again during pressure-throttling of the reduced orifice area.

(C) It would probably not be difficult to extend the range over which this injector (originally designed for constant-thrust operation) could be pressure/area-step throttled at c^* efficiencies above 95%. One way would be to allow initially-higher injection velocities (and therefore injection pressure drops) at full thrust so that a greater range of ϕ could be spanned before the velocities got low enough to cause performance degradation. Another way would be to shut off even more elements during the area step-change and reduce the orifice diameters of those that remained on, which would also maintain high injection velocities. Based on chamber pressure measurements, 6-to-1 throttling at c^* efficiencies in excess of 95% has actually been reported (Ref. 22) with an impinging-jet injector specifically designed for pressure/area-step throttling.

B. Performance During Simulated Discrete-Element Throttling

(U) Characteristic velocity efficiency, chamber pressure, and injection pressure drop are plotted vs the throttle ratio ϕ in Figs. 16–18 for those tests (Nos. 24, 26, 28, and 30 in Table 3) in which simulated discrete-element throttling was carried out at a constant supply pressure of 220 psia (both fuel and oxidizer). The points shown for the 27- and 42-element configurations were obtained by interpolation from the 42-element firings of Table 2 and the 27-element firings of Table 3, to get η_{c^*}'s and ϕ's corresponding to a 220 psia supply pressure. Continuous curves have been

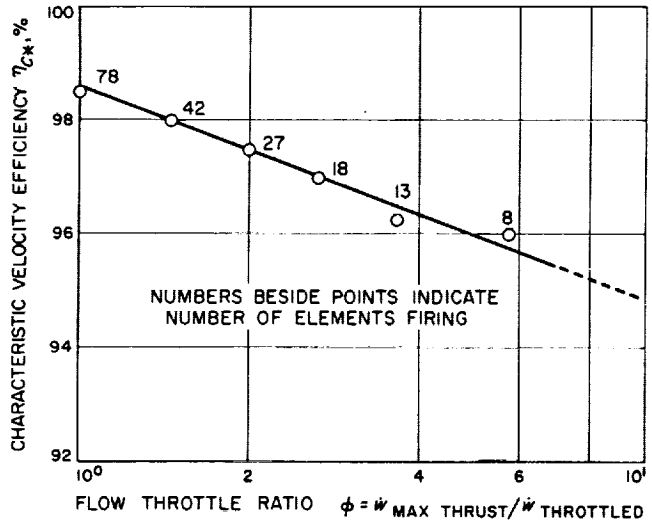

(C) Fig. 16. Variation of c^* efficiency during discrete-element throttling at constant supply pressure

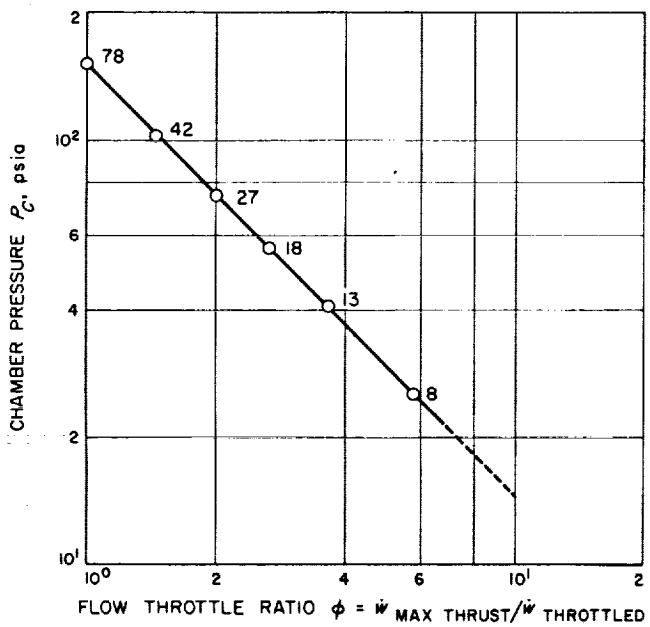

(U) Fig. 17. Variation of chamber pressure during discrete-element throttling at constant supply pressure

drawn through the points mainly to illustrate data trends and consistency, but it should be kept in mind that all actual variations would be stepwise if the numbers of elements firing were restricted to integers. The graphs may be used to illustrate how these key parameters vary

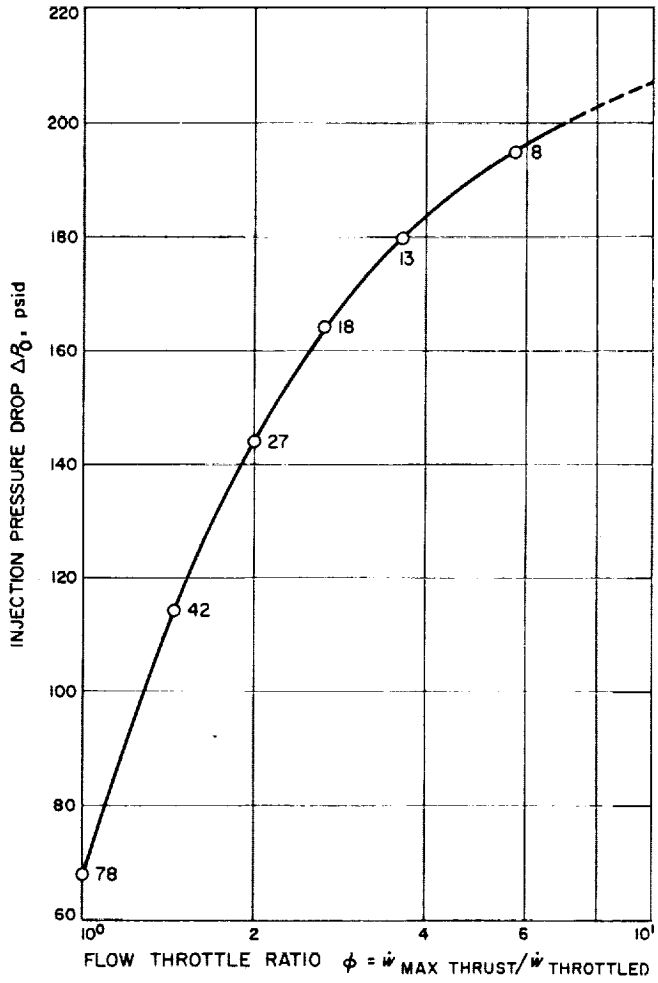

(U) Fig. 18. Variation of injection pressure drop (fuel or oxidizer) during discrete-element throttling at constant supply pressure

when the engine is throttled by the discrete-element method at constant supply pressure. The numbers next to the data points indicate how many elements were fired in each case. For pattern arrangements, refer to Fig. 10.

(C) Examination of Fig. 16 will show that c^* efficiencies of about 98.5% were realized at full thrust (78 elements firing, throttle ratio of 1.0), and that these declined gradually to 96% at a throttle ratio of 5.75. The extrapolation of the curve of Fig. 16 to $\phi = 10$ seems reasonable, and indicates the possibility of throttling to that extent without η_{c^*} falling below about 95%, provided, of course, that chamber pressure does not fall below the vapor pressure of the oxidizer. Chamber pressure decreased almost linearly as the throttle ratio increased, since the combustion efficiency was nearly constant ($P_c = c^*\dot{w}_t/A_t g_c$), as

shown in Fig. 17. Injection pressure drops *increased* with throttling (Fig. 18), asymptotically approaching the supply pressure. This is because the chamber pressure decreased while the injection pressure remained constant.

(C) The throttle ratio ϕ vs the number of elements firing is plotted in Fig. 19, strictly as a matter of convenience. Extrapolation of this curve indicates that shutting off all but four or five of the original 78 elements should result in about 10:1 throttling.

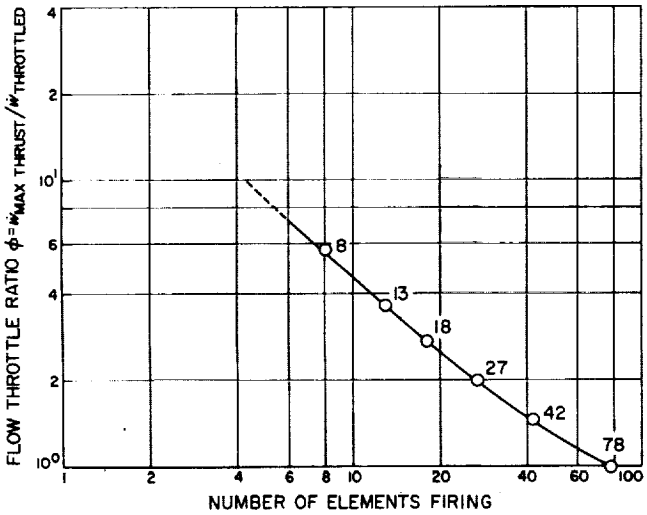

(U) Fig. 19. Throttle ratio as a function of the number of elements firing

C. Comparison of Discrete-Element and Pressure/Area-Step Throttling

(C) In terms of the combustion efficiency levels attained during the throttling of the impinging-sheet injector by the two methods, it appears that discrete-element throttling offers a somewhat greater throttle range (at least 6.0 compared to 3.75) than the pressure/area-step technique if η_{c^*} is to be maintained above 95%. However, the pressure area-step technique cannot be considered *inherently* inferior to the discrete-element method, since the present injector was designed as a fixed-thrust device, and therefore did not incorporate some of the design modifications that have been found (Ref. 22) to extend the range of pressure/area-step throttling. No attempt was made to optimize the pattern arrangements or orifice sizes used with each of the two flow areas separated by the step-change.

(U) For discrete-element throttling, further studies would be required to determine the optimum-element shutoff program. For example, the largely arbitrary patterns used for test purposes (Fig. 10) are not necessarily optimum with regard to maintaining a maximum amount of secondary propellant mixing between the sprays from adjacent elements. For these reasons, it is not possible to draw general conclusions as to which throttling technique is more effective. The feasibility of both techniques has been demonstrated with a multiple-element impinging-sheet injector, and it is highly probable that further development could improve the high-performance throttle range of each.

(C) It is possible, however, to anticipate some generic advantages and problem areas to be expected with each technique. One of the advantages of the pressure/area-step throttling method could be the relatively smooth and continuous variation of thrust and chamber pressure, and the essentially constant c^* efficiency, even across the area step-change. On the other hand, the smooth transition between the two different flow areas noted in the present work probably resulted from the unique near-constancy of c^* efficiency during pressure-throttling exhibited by the impinging-sheet injection elements. The curves of chamber pressure, thrust, and c^* efficiency obtained by other investigators (Ref. 22) for the pressure/area-step throttling of impinging-jet elements have large discontinuities because of the pronounced effects of injection velocity on the performance of impinging-jet elements. A second advantage of this technique could derive from the relatively large number of elements (nominally about half) that remain *on* after the area step-change. This helps to preserve any programmed mass-flux distributions during thrust reduction, and maintains a high level of secondary mixing. In engine applications involving boundary-layer or fuel-film cooling, this high mass-flux density could be used to promote a partial reaction of the central spray core with a fuel film on the walls, thus augmenting performance. Finally, the set of dual manifolds integral with the injector body could help to cool it, so that the pressure/area-step technique might be favored for applications requiring continuous firings of long duration.

(C) However, there are a number of disadvantages to this method. One is the limited range over which throttling can probably be accomplished without performance degradation. Even a judicious selection of the exact location of the area step-change point, or the use of smaller areas and higher velocities for low-thrust operation, would not be expected to extend the nearly-constant-performance throttle range much beyond about 6:1. This is because injection velocities decrease during pressure-

throttling, and eventually become so low as to degrade performance. A second and more serious drawback is that, at the moment the area step-change is made, two on-off valves must close and two pressure-throttling valves must go from a nearly-closed to a full-open position. This is almost certain to affect the dynamic response attainable and would probably result in a rather complex control system if sporadic behavior at the area transition point is to be avoided. It is recognized that some of these difficulties might be circumvented by modifications to the basic scheme. For example, the dual propellant manifolds could be throttled independently. Nevertheless, the dual manifolds, and whatever combination of on-off and pressure-throttle valves is finally used, could add considerably to the weight and complexity of the propulsion system.

(C) Perhaps the most striking advantage of the discrete-element throttling method is the potentially wider range over which throttling could be accomplished at high and essentially constant performance efficiencies. Since injection velocities increase during thrust reduction, they could keep the combustion efficiencies of the individual elements high. In addition, both the on-off and intermediate throttling functions could be accomplished with a single valve package, which could eliminate heavy and voluminous manifolding by feeding each injection element directly.

(U) Among the disadvantages of discrete-element throttling must be included the fact that flowrate, chamber pressure, and thrust will not vary continuously during throttling. Rather, the curves of these parameters vs throttle ratio would consist of a number of discrete steps or increments, corresponding to the opening (or closing) of each new group of orifices by the throttle valve. With a very large number of elements, of course, continuous curves are approached in the limit. The steps calculated for the present 78-element injector are quite small, even when closing off the orifices in groups of five. However, one can envision injectors with very few elements, each contributing a large fraction of the total thrust, in which the steps would be so large that discrete-element throttling would probably not be competitive with other techniques.

(U) Another disadvantage, and one which may provide the ultimate limit to the high-performance throttle range attainable, is the inevitable decrease in the amount of secondary mixing possible between the sprays of adjacent elements, as more and more elements are shut off, leaving those remaining on more widely separated. No injection element has yet been found which can create a totally uniform mixed spray of propellants. Consequently, all injector designs must depend to some degree on secondary spray interactions to promote additional mixing. Aside from this, there should be no objection to progressively shutting off more and more elements during throttling, since neither a uniform nor a hump-type distribution seems absolutely necessary for efficient, stable combustion with this injector.

D. Effects of Chamber Length, Mixture Ratio and Propellant Combination on Combustion Efficiency

(U) The experimental results reported in Tables 4 and 5 are plotted against a normalizing parameter $\mathscr{R}$ in Fig. 20, where

$$\mathscr{R} = (1 + \theta)^{-1} \tag{4}$$

and θ is the stream momentum flux ratio divided by the orifice diameter ratio,

$$\theta = \frac{m_f/m_o}{d_f/d_o} \tag{5}$$

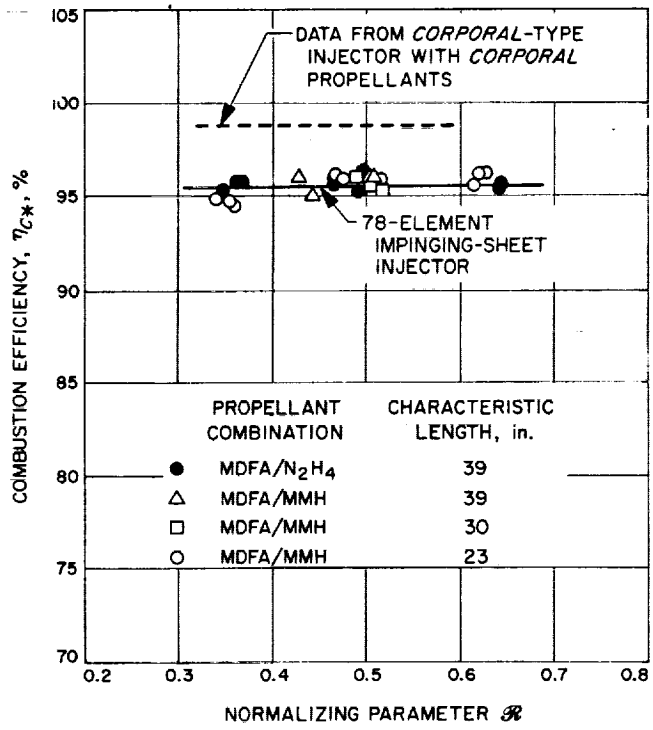

(C) Fig. 20. Combustion efficiency vs normalizing parameter (Ref. 13) for multiple-element impinging-sheet and impinging-jet injectors

First introduced in Ref. 13 as

$$\theta = \frac{\rho_f V_f^2 d_f}{\rho_o V_o^2 d_o} \tag{6}$$

it may also be expressed in the equivalent form,

$$\theta = \left(\frac{1}{r}\right)^2 \left(\frac{\rho_o}{\rho_f}\right) \left(\frac{d_o}{d_f}\right)^3 \tag{7}$$

$\mathcal{R}$, a function of liquid physical properties, injection velocity, and injector geometry, has been useful in correlating the mixing of nonreactive propellant simulants (Ref. 13) and the combustion efficiency attained in actual firings of unlike-doublet jet injectors (Ref. 23).

(C) Over the range of $\mathcal{R}$ studied, corresponding to mixture ratios from 1.0 to 1.8 for MDFA/N_2H_4 and MDFA/MMH, η_{c^*} remained essentially constant and fairly high (95 to 96%) despite variations in injection velocities from 34 to 92 ft/s. Both propellant combinations gave essentially the same combustion efficiency, and characteristic length changes in the range $23 \leq L^* \leq 39$ in. did not appreciably influence performance. Chamber pressure had no noticeable effect on η_{c^*}. The high performance noted in the N_2O_4/N_2H_4 firings of Tables 2 and 3 was therefore inherent in the basic injector design and did not result solely from the large values (39 in.) of characteristic chamber length originally used.

(C) These results indicate that for the 78-element impinging-sheet injector, combustion efficiency is very insensitive to both injection velocity and $\mathcal{R}$, for $0.35 \leq \mathcal{R} \leq 0.65$, but this behavior is not necessarily unique to multiple-element impinging-sheet injectors. For purposes of comparison, data from a 52-element *Corporal*-type unlike-doublet impinging-*jet* injector[3] have also been plotted in Fig. 20. Over almost the same range of $\mathcal{R}$ the performance-efficiency of the impinging-jet injector, which featured a degree of hydraulic control and reproducibility comparable to that of the sheet injector, also remained constant. (Absolute efficiency levels cannot be directly compared because of differences in propellants, chamber pressure, characteristic length, measurement techniques, and data reduction).

(C) These results show comparable insensitivity of η_{c^*} to $\mathcal{R}$ for $0.35 \leq \mathcal{R} \leq 0.65$ with both kinds of injectors; in this range, impinging-sheets are therefore fully competitive with impinging-jets. In these multi-element injectors, this insensitivity may be due in some measure to secondary mixing effects brought about by interactions between adjacent spray fans. However, the behaviors of *single* impinging-jet and impinging-sheet elements are quite different. The liquid-phase mixing of a pair of nonreactive unlike-impinging-sheets was reported in Ref. 8 to be manifestly insensitive to stream momentum ratio. However, that of a pair of nonreactive unlike-impinging-jets (Ref. 13) varied markedly with momentum ratio, with the propellant mixing factor E_m exhibiting a sharp peak at a value of momentum ratio equal to the diameter ratio of the jets. This would indicate less sensitivity of local mixing (consequently, performance efficiency) to variations in mixture ratio with impinging-sheet injectors, especially in small injectors consisting of relatively few elements, in which case the favorable effects of secondary mixing are felt to a lesser degree.

(C) As noted earlier, the N_2O_4/N_2H_4 propellant combination gave typical c^* efficiencies on the order of 98.5%. It would be expected that MDFA/N_2H_4 and MDFA/MMH, which are chemically similar, should give about the same combustion efficiency as N_2O_4/N_2H_4 when fired with the same injector and chamber. However, c^* efficiencies of only 95 to 96% were realized with the maximum density acid combinations. One possible explanation for this apparent difference in combustion efficiencies may lie in the theoretical values of characteristic velocity used in calculating the c^* efficiencies. There is considerable doubt as to the validity of the heat of formation (−30.413 kcal/mole) used for the MDFA in the theoretical performance calculations. Thus, the theoretical values of c^* may be somewhat high, and the actual values of η_{c^*} based on them may be one or two percentage points higher than those reported here.

(C) Another potential cause of the discrepancies in combustion efficiency noted with the different oxidizers may lie in chemical differences between them, resulting in slight differences in the mechanisms of mixing and atomization prevailing in the reactive environment. A third possible cause of the observed difference in combustion efficiency may be the difference in surface finish (see Fig. 2) between the steel and molybdenum deflectors. The N_2O_4/N_2H_4 firings were all carried out with the original steel deflectors, but enough of these were rendered unserviceable in the throttling experiments to require refurbishing of the injector with a new complement of deflectors prior to the MDFA test series. These were

[3](U) Rupe, J. H., private communication, Nov. 8, 1967.

the molybdenum devices with the pitted surface characteristic of electrodischarge machining. It is highly unlikely that these surface differences, undetectable to the naked eye, could account for a nearly 2% degradation in combustion efficiency, and the discrepant heat of formation remains the most probable explanation. In any event, this work has demonstrated that combustion efficiencies in excess of 95% are certainly attainable with the maximum density nitric acid when used with several fuels of the hydrazine family.

E. Heat Transfer

(C) The local gas-side heat-transfer coefficients (calculated from Eqs. (1) and (2) are plotted vs circumferential position around the combustion chamber (Fig. 21) for those tests in which all 78 elements were fired. Data appear in alternating quadrants because the chamber was rotated to a second position during some firings. There is negligible variation in this coefficient with circumferential position over the range of chamber pressures for which heat-transfer measurements were made (79–154 psia). This uniformity is attributed to the radially-oriented spray fans (see Fig. 6).

(U) The corresponding gas-side coefficients for Test No. 10 of Table 2, in which 33 of the elements were "turned off," resulting in the spray-fan pattern of Fig. 8, are plotted vs circumferential position to an enlarged scale in Fig. 22. As was expected, a slight variation with position was noted in the coefficient. This variation can be correlated with the injector spray pattern. For example, the "peak" heat-transfer coefficients at A and B in Fig. 22 occur at the locations of maximum mass-flux density near the wall (the ends of the spiral arms A and B in Fig. 8). Similar results would probably have been found in the remaining firings had their durations been long enough to permit accurate heat-flux measurements.

(U) Circumferential variations in the heat-transfer coefficient are closely related to the orientation of the injector spray fans, especially those nearest the chamber periphery. The results are in agreement with similar observations made in Ref. 2 and elsewhere. It may be noted that the measured values of h_g were slightly higher than those calculated by the semi-empirical equation (Ref. 24), which is sometimes used to estimate rocket-nozzle heat-transfer coefficients in the absence of experimental data.

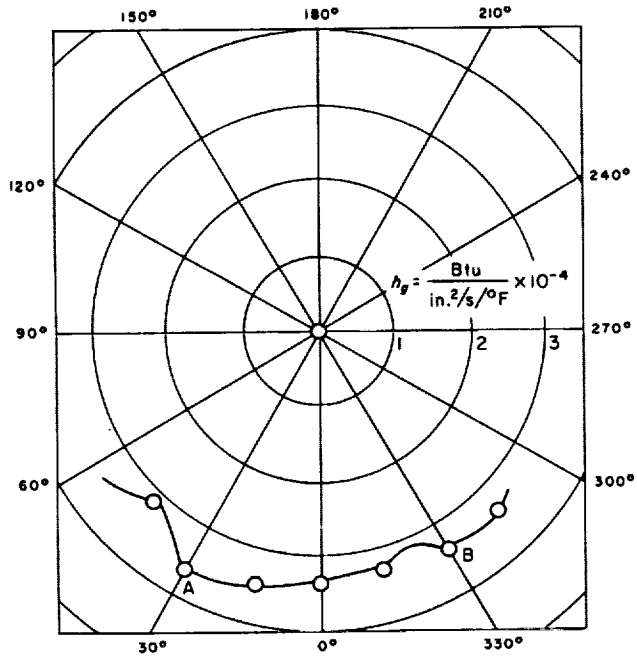

(C) Fig. 21. Variation of heat-transfer coefficients around chamber circumference at various chamber pressures (all 78 elements firing)

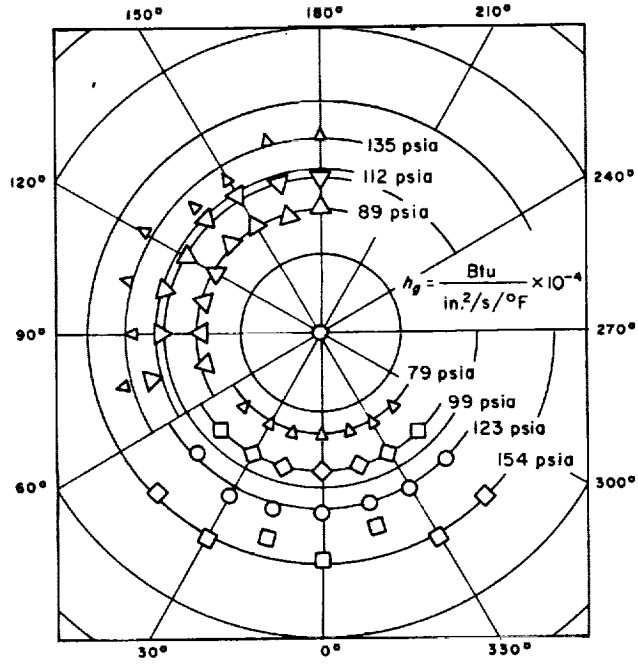

(U) Fig. 22. Variation of heat-transfer coefficients around chamber circumference at 93-psia chamber pressure, 45 elements (pattern of Fig. 8) firing

F. Durability of Injection Elements

(U) The experimental results with the steel deflectors indicate that injector durability can present a major problem when an impinging-sheet injector with externally-mounted elements is throttled by *any* technique that involves the shutting off of a number of elements. To prolong the life of such exposed elements, a flow of propellant on each deflector may well be necessary. To afford them a greater measure of thermal protection, it may be necessary in future designs to recess the elements within the face of the injector, perhaps even those elements made of refractory or more highly-conductive materials.

(U) The work of Ref. 25 showed that impinging-sheet injection elements *could* be buried within an injector face with no loss in delivered c^* efficiency compared to an external installation, provided that suitable means were provided to vent the internal cavity between the deflectors. Without such venting, serious performance degradation resulted. The cause was attributed to the disruption of the impingement process by escaping combustion gases from the reactive backspray of propellants emanating from the impinging sheets. These firings, however, were also of short (1–5 s) duration, and as yet, there is no direct experimental evidence to confirm the contention that buried deflectors will be more durable than exposed ones. By analogy with round orifices buried within an injector face (a commonly-used configuration), it seems likely that they would be. Recessed elements may actually be required, even when none are shut off, especially with the higher-energy space-storable propellants, where any external deflectors, even those flowing propellants, are exposed to a severe convective and radiative heat-transfer environment. The short durations of even those tests in which all 78 elements were flowing full, were not sufficient to permit firm conclusions to be drawn regarding the long term durability of elements exposed to an N_2O_4/N_2H_4 combustion environment. Deflector damage could conceivably have been sustained in these tests had the combustion chamber design permitted longer duration firings.

(U) A metallurgical examination of a representative sampling of the failed molybdenum deflectors indicated the failure mode to have been brittle fracture of the molybdenum. The bar stock from which the parts were fabricated was extremely anisotropic. A longitudinal section through a piece of as-received stock is shown in Fig. 23 (a) to 100× magnification (after etching with Murakami's reagent). The electrodischarge-machining process, which sometimes produces a highly-stressed skin effect in steels, apparently had no effect on the molybdenum, as illustrated by an unfired deflector in Fig. 23 (b). Similarly, the 25 injector firings did not seem to exert any deleterious thermal effects on the microstructure of the deflectors, as evidenced by the photomicrograph of Fig. 23 (c). A microhardness survey, comparing fired and unfired sections, confirmed this finding. Failure of the deflectors was therefore attributed to the inherently brittle microstructure of the as-received molybdenum, which was insufficient to resist the high, transient shear-loadings imposed by overpressurization during the hard starts.

(U) These results suggest that extreme caution should be exercised when using potentially brittle, refractory materials for injector or thrust-chamber fabrication. Even though they have desirable thermal properties, they may be mechanically unsatisfactory. To assure that brittle transitions do not occur, sufficient control should be maintained over the properties of as-received stock, as well as over the conditions of brazing, welding, or heat-treating processes.

G. Smoothness and Stability of Combustion

(C) As far as can be determined from an examination of the archives at JPL, the combustion of N_2O_4 and N_2H_4 with the present impinging-sheet injector is the smoothest yet attained at a scale greater than ~100 lbf thrust. This is considered a signicant improvement, because hydrazine combustion with many conventional injectors is often characteristically rough. This may be related to the fine atomization and relatively uniform mixing that cold flow measurements indicate are typical of such impinging-sheet devices. This explanation is somewhat strengthened by recent results with so-called "micro-orifice" injectors, which also achieve superior propellant mixing and atomization. When fired with N_2O_4/N_2H_4 (Ref. 26), these injectors yielded chamber-pressure traces as smooth as those obtained with N_2O_4/MMH, even as did the impinging-sheet injector in the present program.

(U) Any discussion of combustion stability must be restricted to the lack of observable "spontaneous" instabilities. The dynamic response of this particular injector/chamber combination was not determined, because the number of molybdenum deflectors lost through brittle failure precluded carrying out the planned bomb tests. Similarly, it cannot be said with certainty that the lack of spontaneous instabilities resulted *solely* from the hump-type mass-flux distribution. Actually, during the discrete-element throttling tests, this distribution was progressively

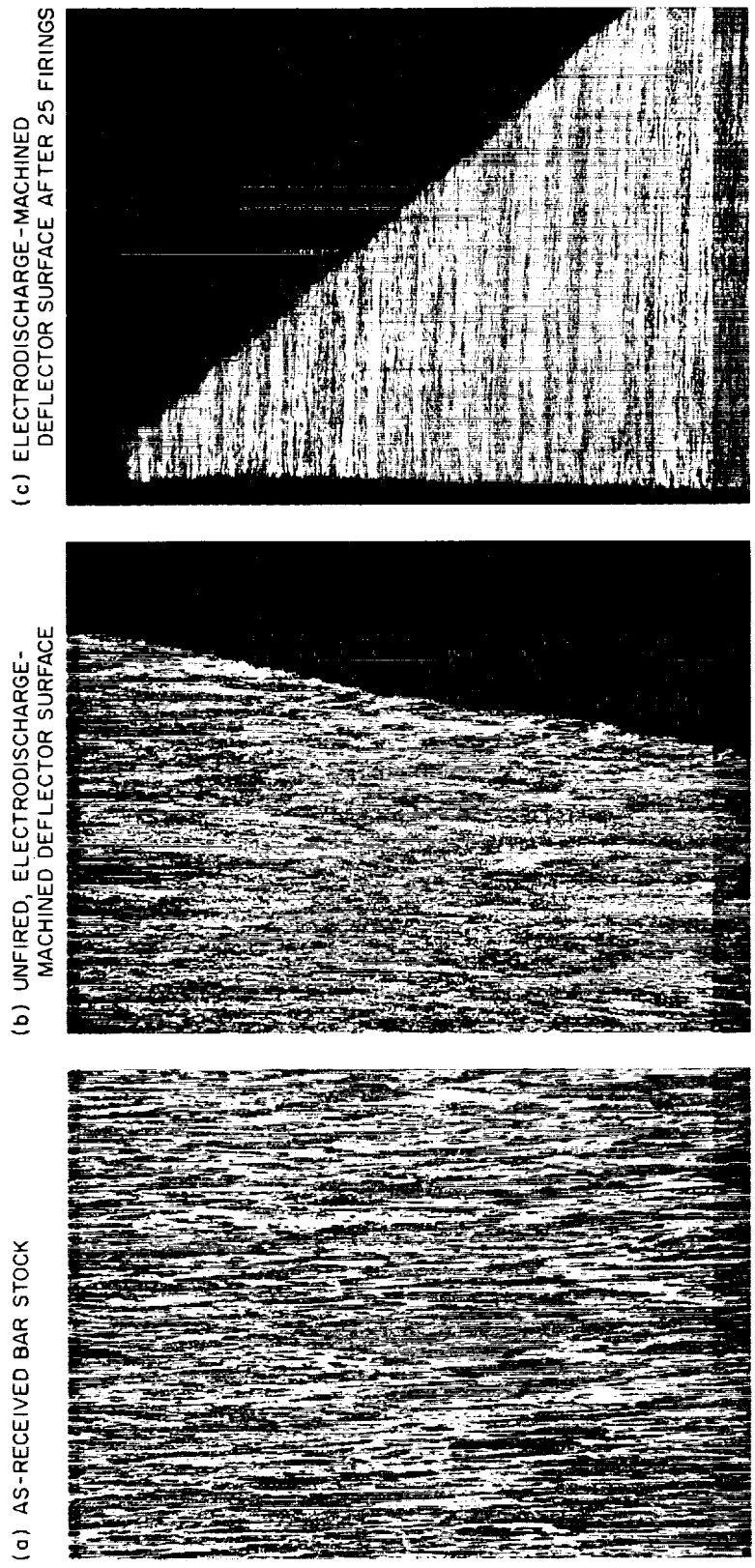

(U) Fig. 23. Photomicrographs of TZM molybdenum stock and deflector surfaces

altered without any noticeable effects on stability. However, the high performance registered when the hump-distribution was used indicates that it has no *adverse* effects on combustion efficiency.

VII. Summary of Results

(C) The results of this experimental program have demonstrated the feasibility of JPL's impinging-sheet injection elements. The multiple-element injector yielded c^* efficiencies as high as 98.5% when operated under full-thrust flowrates, an achievement at least as good as any performances obtained with multiple-element, impinging-jet devices. The feasibility of throttling the impinging-sheet injector over reasonably wide ranges, without combustion efficiency falling below about 95%, was demonstrated for two candidate throttling techniques: the pressure/area-step and discrete-element methods. Throttle ranges of about 4:1 and 6:1 (at $\eta_{c^*} \geq 95\%$) were established for these two methods respectively, even though the injector had originally been designed for fixed-thrust operation. The potential of extending the high-performance throttle ranges of both techniques by suitable injector optimization was also indicated. In addition, the capability of the impinging-sheet injector to operate at propellant mixture ratios considerably different from the design value, without any appreciable degradation in combustion efficiency, has been proven. There were no instances of combustion instability.

(U) The durability of externally-mounted injection elements proved to be a major problem area, especially for those elements deprived of a cooling flow of propellants by being shut off during throttling. Their fabrication, however, was relatively simple and inexpensive because of the application of electrodischarge-machining techniques.

(U) Maximum density fuming nitric acid (MDFA), evaluated as an alternate oxidizer because of its improved density and vapor pressure under sterilization cycle conditions, was found to be competitive with N_2O_4 as to efficiency, stability, and smoothness of combustion.

VIII. Conclusions

(C) Multiple-element, unlike-impinging-sheet injectors of the type evaluated in this study are competitive with contemporary impinging-jet injectors as to combustion efficiency, stability, and smoothness, when fired with N_2O_4/N_2H_4 in chambers of reasonable ($L^* \geq 23$) length. Furthermore, without appreciable degradation in combustion efficiency, they may be throttled over a fairly wide range (at least as high as 6:1), operated over wide excursions in mixture ratio, and fired with other propellants in the earth-storable (oxides of nitrogen–hydrazine) family.

(U) Due to the relatively poor durability of externally-mounted injection elements, especially during throttling, it would seem desirable to concentrate future development efforts on means of "burying" the elements within the face of the injector. In this way, the elements can be afforded greater thermal protection.

(U) Nomenclature

A_t throat area

c^* characteristic velocity, ft/s

C_F thrust coefficient (dimensionless)

d_f orifice diameter of fuel

d_o orifice diameter of oxidizer

E_m propellant mixing factor (see Ref. 13)

F thrust, lbf

G local mass flux per unit area

g_c gravitational constant, 32.174 ft/s^2

h_g gas-side heat transfer coefficient, $\frac{\text{Btu}}{\text{in.}^2/\text{s}/^\circ\text{F}}$

L^* characteristic length of chamber, in.

m_f fuel stream momentum flux

m_o oxidizer stream momentum flux

P_a ambient (sea level) pressure

P_c chamber pressure, psia

q/A heat flux, $\frac{\text{Btu}}{\text{in.}^2/\text{s}}$

$\mathcal{R}$ normalizing parameter

r oxidizer/fuel mixture ratio

T_c theoretical combustion temperature, °F

T_o driving-gas (stagnation) temperature, °F

T_w temperature at the wall, °F

V velocity, fps

V_f fuel velocity, fps

V_o oxidizer velocity, fps

$\dot{w}$ flowrate, lbm/s

$\dot{w}_t$ total flowrate, lbm/s

Δp_f fuel injection pressure drop, psid

Δp_o oxidizer injection pressure drop, psid

ϵ_c contraction area ratio

ϵ_e expansion area ratio

η_{c^*} characteristic velocity efficiency, % (combustion efficiency)

θ stream momentum flux ratio divided by the orifice diameter ratio

ϕ flow throttle ratio

ρ_f liquid density of fuel, lbm/ft^3

ρ_o liquid density of oxidizer, lbm/ft^3

(U) References

1. Rupe, J. H., and Evans, D. D., "Designing for Compatibility in High-Performance Liquid Propellant Engines, *Astronaut. Aeronaut.*, Vol. 3, No. 6, p. 68, June 1965.

2. Rowley, R. W., and Tyler, W. H., *The Effect of Injector Design on Thrust-Chamber Erosion,* Technical Report 32-750. Jet Propulsion Laboratory, Pasadena, Calif., Mar. 1, 1966.

3. Rupe, J. H., and Jaivin, G. I., *The Effects of Injection Mass Flux Distributions and Resonant Combustion on Local Heat Transfer in a Liquid-Propellant Rocket Engine,* Technical Report 32-648. Jet Propulsion Laboratory, Pasadena, Calif., Oct. 1, 1964.

4. Conn, T. E., Hester, J. N., and Valentine, R. S., "Environmental Effects Upon Rocket Injector/Chamber Compatibility," *J. Spacecraft Rockets,* Vol. 4, No. 12, p. 1581, Dec. 1967.

5. Harrje, D. T., "Fundamental Problems of Injector Design," presented at 25th AGARD Colloquium on Advances in Tactical Rocket Propulsion, University of California, San Diego, Calif., Apr. 1965.

6. Riebling, R. W., *The Formation and Properties of Liquid Sheets Suitable for Use in Rocket Engine Injectors,* Technical Report 32-1112. Jet Propulsion Laboratory, Pasadena, Calif., June 15, 1967.

7. Riebling, R. W., "Controlling the Dimensions and Orientation of Impinging Propellant Sheets in Liquid Rocket Engine Injectors," *J. Spacecraft Rockets,* Vol. 3, No. 11, p. 1692, Nov. 1966.

8. Riebling, R. W., "The Liquid-Phase Mixing of a Pair of Impinging Sheets," in *Supporting Research and Advanced Development,* Space Programs Summary 37-48, Vol. III, p. 135. Jet Propulsion Laboratory, Pasadena, Calif., Dec. 31, 1967.

9. Riebling, R. W., *The Current State of Impinging-Sheet Injector Technology,* CPIA Publication No. 155, Vol. II. Chemical Propulsion Information Agency, Johns Hopkins University, Silver Spring, Md., Sept. 1967.

10. Evans, D. D., Stanford, H. B., and Riebling, R. W., *The Effect of Injector-Element Scale on the Mixing and Combustion of Nitrogen Tetroxide-Hydrazine Propellants,* Technical Report 32-1178. Jet Propulsion Laboratory, Pasadena, Calif., Nov. 1, 1967.

11. Evans, D. D., "Injector Development," in *Supporting Research and Advanced Development,* Space Programs Summary 37-35, Vol. IV, p. 152. Jet Propulsion Laboratory, Pasadena, Calif., Oct. 31, 1965.

12. Evans, D. D., "Injector Development," in *Supporting Research and Advanced Development,* Space Programs Summary 37-34, Vol. IV, p. 174. Jet Propulsion Laboratory, Pasadena, Calif., Aug. 31, 1965.

13. Rupe, J. H., *A Correlation Between the Dynamic Properties of a Pair of Impinging Streams and the Uniformity of Mixture Ratio Distribution in the Resulting Spray,* Progress Report 20-209. Jet Propulsion Laboratory, Pasadena, Calif., Mar. 28, 1956.

(U) References (contd)

14. Powell, W. B., Howell, G. W., and Irving, J. P., *A Method for the Determination of Local Transient Heat Flux in Uncooled Rocket Motors*, Technical Report 32-257. Jet Propulsion Laboratory, Pasadena, Calif., July 1, 1962.

15. Riebling, R. W., et al., *Interim Report, Chamber Technology for Space-Storable Propellants—Task II*, Vol. II, Report R-0628-2. Rocketdyne, Canoga Park, Calif., Oct. 13, 1965.

16. Riebling, R. W., et al., "Experimental Evaluation of the Performance of a Concentric-Tube Throttling Injector," presented at 7th Liquid Propulsion Symposium, Denver, Colorado, Oct. 19, 1965.

17. *Dual Manifold Injector Advancement Program, Final Report*, Report UTC 2155-FR. United Technology Corp., Sunnyvale, Calif., Dec. 31, 1966.

18. Green, W. J., et al., *Liquid Throttle Engine Program*, Report LF-0981-00-1. Aerojet-General Corp., Sacramento, Calif., Apr. 1966.

19. Mitchell, J. P., et al., *Advanced Throttling Concepts Study*, Report PWA FR-1108. Pratt & Whitney Aircraft, W. Palm Beach, Fla., Sept. 15, 1964.

20. Riebling, R. W., and McDougal, A. R., "Propellant Valve Development," in *Supporting Research and Advanced Development*, Space Programs Summary 37-49, Vol. III, p. 236. Jet Propulsion Laboratory, Pasadena, Calif., Feb. 29, 1968.

21. *Performance and Properties of Liquid Propellants*, Report LRP 178. Aerojet-General Corp., Sacramento, Calif., July 13, 1960.

22. *Third Interim Report, Chamber Technology for Space Storable Propellants*, Report R-7073 (Contract No. NAS7-304). Rocketdyne, Canoga Park, Calif., May 31, 1967.

23. Falk, A. Y., and Barsic, N., *Injector Design Criteria Applicable to Internal Regenerative (INTEREGEN) Cooled Rocket Engines*, Report RR67-1. Rocketdyne, Canoga Park, Calif., Jan. 1967.

24. Bartz, D. R., "A Simple Equation for Rapid Estimation of Rocket Nozzle Convective Heat Transfer Coefficients," *Jet Propulsion*, p. 49, Jan. 1957.

25. Riebling, R. W., "Injector Development: Impinging-Sheet Injectors," in *Supporting Research and Advanced Development*, Space Programs Summary 37-44, Vol. IV, p. 182. Jet Propulsion Laboratory, Pasadena, Calif., Apr. 30, 1967.

26. McGough, C. B., La Botz, R. J., and Addoms, J. F., "Development of HYPERTHIN Injectors for Reaction Control Thrustor Application," Presented at ASME 1968 Aviation and Space Conference, Los Angeles, Calif., June, 1968.